The Texas Medical Center Library
DigitalCommons@TMC

Dissertations and Theses (Open Access)

MD Anderson UTHealth Houston Graduate School

5-2014

Anti-Insulin Resistance Treatments Suppress Her2+ Breast Cancer Growth Via Altering Metabolism

PING-CHIEH CHOU

Follow this and additional works at: https://digitalcommons.library.tmc.edu/utgsbs_dissertations

Part of the Cancer Biology Commons, and the Medicine and Health Sciences Commons

Recommended Citation

CHOU, PING-CHIEH, "Anti-Insulin Resistance Treatments Suppress Her2+ Breast Cancer Growth Via Altering Metabolism" (2014). *Dissertations and Theses (Open Access)*. 450.
https://digitalcommons.library.tmc.edu/utgsbs_dissertations/450

This Dissertation (PhD) is brought to you for free and open access by the MD Anderson UTHealth Houston Graduate School at DigitalCommons@TMC. It has been accepted for inclusion in Dissertations and Theses (Open Access) by an authorized administrator of DigitalCommons@TMC. For more information, please contact digcommons@library.tmc.edu.

The TMC LIBRARY Health Sciences Resource Center

ANTI-INSULIN RESISTANCE TREATMENTS SUPPRESS HER2^{+} BREAST CANCER GROWTH VIA ALTERING METABOLISM

by

Ping-Chieh Chou, B.S., M.S.

APPROVED:

_____

Mong-Hong Lee, Ph.D., Supervisory Professor

_____

Min Gyu Lee, Ph.D.

_____

Hui-Kuan Lin, Ph.D.

_____

Dos Sarbassov, Ph.D.

_____

Sai-Ching Jim Yeung, M.D., Ph.D.

APPROVED:

_____

Dean, The University of Texas

Graduate School of Biomedical Sciences at Houston

ANTI-INSULIN RESISTANCE TREATMENTS SUPPRESS HER2^{+} BREAST CANCER GROWTH VIA ALTERING METABOLISM

A

DISSERTATION

Presented to the Faculty of

The University of Texas

Health Science Center at Houston

and

The University of Texas

MD Anderson Cancer Center

Graduate School of Biomedical Sciences

in Partial Fulfillment

of the Requirements

for the Degree of

DOCTOR OF PHILOSOPHY

by

Ping-Chieh Chou, B.S., M.S.

Houston, Texas

May, 2014

DEDICATION

This dissertation is dedicated to all the people who have encouraged me to pursue this degree. I want to thank my parents for supporting me unconditionally. I especially want to dedicate my work to my grandfather, Chao Chu, who passed away because of prostate cancer. He is my inspiration and driving force. Most of all, I dedicate this dissertation to my wife, Sylvia Chen, who simply completes my life.

ACKNOWLEDGEMENTS

I would like to first acknowledge my mentor, Dr. Mong-Hong Lee, for the opportunity to pursue my degree in his laboratory. As a mentor, he not only provides his guidance in science, but also shares his wisdom about life. He teaches me to think positively, to have the right concept about everything, and to be grateful for the things we already have. I feel really lucky to be his student learning how to be a good scientist and a better person in the past few years.

I also would like to show my appreciation to my co-mentor, Dr. Sai-Ching Jim Yeung, for giving me critical advice and ideas. Dr. Yeung is my role model as the amazing medical doctor, scientific researcher, and statistic expert in the laboratory. He brings the benchwork more closely to the clinical bed side and shows me that research can be challenging and fun.

I would like to thank Dr. Michelle Barton, Dr. Maria-Magdalena Georgescu, Dr. Suyun Huang, Dr. Min Gu Lee, Dr. Randy Legerski, Dr. Hui-Kuan Lin, Dr. Lalitha Nagarajan, Dr. Jenet Price, Dr. Dos Sarbassov, Dr. Michael Van Dyke, and Dr. Keping Xie who have served in my committee and given suggestions and help.

I would like to thank Dr. Yun Wu, Dr. Jim Bankson, and Dr. Jae Hyuk Lee for their professional and technical help. I thank Dr. Ruiying Zhao for giving me the

chance to continue the project the she initiated. I would like to thank all the members in Dr. Lee's laboratory. It is a very good experience to have this journey with you.

Finally, I would like to thank my wife and my two lovely daughters, who bring happiness to my life every day. I would like to thank my mother, a $HER2^{+}$ breast cancer patient and survivor bravely fighting her own cancer right now, becomes a teacher at the end of my Ph.D. training. She shows me all the emotion, stress, anxiety, frustration, pain, worries, and questions as a cancer patient could have and lets me understand that the importance of my research will eventually become a force to end this terrible disease.

ANTI-INSULIN RESISTANCE TREATMENTS SUPPRESS HER2^{+} BREAST CANCER GROWTH VIA ALTERING METABOLISM

Ping-Chieh Chou, B.S., M.S.

Supervisory Professor: Mong-Hong Lee, Ph.D.

Epidemiological studies have identified that type 2 diabetes mellitus (DM2) is a significant risk factor for carcinogenesis and cancer death, including breast cancer. Our previous finding in patients showed that anti-insulin resistance treatments are associated with improved HER2^{+} breast cancer survival of diabetic women. However, there were no transgenic mouse models to study the correlation and explain the detailed mechanism. We generated a mouse model of HER2^{+} breast cancer with DM2 by crossing leptin receptor point mutation (*Lepr* $^{db/+}$) and MMTV-ErbB2 (*neu*) mice. The MMTV-ErbB2/*Lepr* $^{db/db}$ mice had a poor survival rate compared with MMTV-ErbB2/*Lepr* $^{+/+}$ mice, and the log rank test of the Kaplan-Meier analysis showed that they were significantly different (P = 0.0004). In addition, we evaluated the impact of different anti-diabetic medications on cancer-specific survival. MMTV-ErbB2/*Lepr* $^{db/db}$ mice administrated with metformin or rosiglitazone showed improved overall survival, cumulative tumor incidence, and reduced tumor progression. Anti-insulin resistance treatments can also reverse the Warburg effect by reducing lactate/pyruvate ratio through ^{13}C-pyruvate imaging. Cell lines isolated from MMTV-ErbB2/*Lepr* $^{db/db}$ mice also showed reduced levels of both oxygen consumption and lactate production upon metformin treatment. Metformin treatment not only inhibited proliferation and

induced apoptosis in Human HER2^{+} breast cancer cell lines, but also repressed *c-MYC* mRNA expression, increased proteasome-dependent degradation, and reduced the downstream key glycolysis enzyme PKM2. Moreover, anti-insulin resistance treatments dramatically change the microenvironment by reducing serum insulin levels and this systematic effect attenuated the mTOR/AKT signaling pathway in tumor samples from MMTV-ErbB2/*Lepr* $^{db/db}$ mice. Anti-insulin resistance treatments also affected adipokine expression profiles and may reveal potential targets for further research. In conclusion, our results indicate the therapeutic effect of anti-insulin resistance treatments on breast cancer metabolism and this animal model also shed the light on the clinical implications of anti-insulin resistance treatments on HER2^{+} breast cancer patients accompanied with the DM2 condition.

TABLE of CONTENTS

APPROVAL SHEET i

TITLE PAGE ii

DEDICATION iii

ACKNOWLEDGEMENTS iv

ABSTRACT vi

TABLE of CONTENTS viii

LIST of FIGURES xii

LIST of TABLES xiv

CHAPTER 1. INTRODUCTION 1

1.1 General background of diabetes mellitus 1

1.1.a Categorization of diabetes mellitus 2

1.2 General background of breast cancer 5

1.3 Diabetes treatments, insulin levels, and anti-cancer effects 11

1.3.a Metformin 12

1.3.b Rosiglitazone 13

1.3.c Anti-insulin resistance treatments and $HER2^{+}$ cancer 15

1.4 Gap in knowledge 16

CHAPTER 2. MATERIAL and METHODS 17

2.1 Mouse Tumor Model 17

2.2 Genotyping, Weight Measurement, Oral Glucose Tolerance Tests and Insulin Tolerance Tests 17

2.3 Mammary Gland Whole-Mount Staining 19

2.5 Survival Analysis 20

2.6 Histology Staining and Mitosis Count 21

2.7 Cell Lines and Cell Culture 21

2.8 Magnetic Resonance Spectroscopic Imaging 21

2.8.1 ^{13}C Polarization Process 22

2.8.2 MRI Imaging Acquisition 22

2.8.3 Data Processing 23

2.9 Measurement of Oxygen Consumption Rate and Extracellular Acidification Rate in Mouse mammary tumor cells from MMTV-ErbB2/*Lepr*$^{db/db}$ mice 23

2.10 Proliferation assay 24

2.11 Western Blot Analysis 25

2.12 Quantitative Real-Time Polymerase Chain Reaction 25

2.13 Enzyme-linked Immunosorbent Assay 28

2.14 Multiplex Assay 28

2.15 Adipokine Array Analysis 29

2.16 Graphs and Statistical Analysis 30

CHAPTER 3. RESULTS 31

3.1 Generating MMTV-ErbB2/*Lepr*$^{db/db}$ transgenic mouse model 31

3.1 Diabetes promotes breast cancer progression and reduces overall survival in the MMTV-ErbB2/*Lepr*$^{db/db}$ transgenic mouse model 34

3.2 Anti-insulin resistance treatments attenuate tumor progression and improve overall survival in HER2^{+} breast cancer diabetic mouse model 37

3.3 Anti-insulin resistance treatments reduce the cancer metabolism *in vivo* 42

3.4 Metformin treatment reduces mitochondrial respiration capacity and glycolysis *in vitro* 46

3.5 Metformin treatment inhibits proliferation, induces apoptosis, and suppresses cancer metabolism in human HER2^{+} breast cancer cell lines 48

3.6 Anti-insulin resistance treatments reduce systemic insulin level, suppress mTOR/AKT signaling in tumor, and regulate adipokine secretion profiles 53

CHAPTER 4. DISSCUSSION 60

4.1 A successful DM2 HER2^{+} breast cancer transgenic mouse model 60

4.2 Demonstrating the anti-cancer effect of anti-insulin resistance treatments by using clinical relevant concentration 61

4.3 Real-time observation of anti-insulin resistance treatments alter breast cancer metabolism by directly inhibiting oxidative phosphorylation and glycolysis in vitro and in vivo 62

4.4 Metformin treatment inhibits c-MYC mRNA expression and induces c-MYC proteasome degradation 64

4.5 Systematic effect of anti-insulin resistance treatments on breast cancer and microenvironment 65

4.6 Future direction 67

CHAPTER 5. BIBLIOGRAPHY 69

Vita 85

LIST of FIGURES

Figure 1. The five major subtypes of breast cancer and the link to normal human mammary epithelial hierarchy..... 6

Figure 2. Patient relapse survival and overall survival on different breast cancer subtypes..... 8

Figure 3. Scheme of mouse breading..... 18

Figure 4. MMTV-ErbB2; *Lepr*$^{db/db}$ mice have insulin resistance and obesity phenotype..... 33

Figure 5. DM2 promotes breast cancer progression in MMTV-ErbB2; *Lepr*$^{db/db}$ mouse model 35

Figure 6. DM2 reduces overall survival and tumor-free survival in MMTV-ErbB2; *Lepr*$^{db/db}$ mouse model..... 36

Figure 7. Anti-insulin resistance treatments improve overall survival and tumor-free survival in MMTV-ErbB2; *Lepr*$^{db/db}$ mouse model 38

Figure 8. Anti-insulin resistance treatments attenuate tumor progression in MMTV-ErbB2/*Lepr*$^{db/db}$ mice..... 39

Figure 9. Metformin treatments delays tumor progression in MMTV-ErbB2/*Lepr*$^{db/db}$ mice 40

Figure 10. Anti-insulin resistant treatments repress cancer progression in MMTV-ErbB2/*Lepr*$^{db/db}$ mice..... 41

Figure 11. MRI image of tumor localization in a MMTV-ErbB2/*Lepr*$^{db/db}$ mouse..... 43

Figure 12. Anti-insulin resistant treatments reduce cancer metabolism in vivo and in vitro.. 45

Figure 13. Metformin treatment reduces oxygen consumption (OCR) and extra cellular acidification rate (ECAR) in vitro..... 47

Figure 14. Metformin treatment inhibits cell proliferation, increases apoptosis, and suppresses key metabolism regulators in Her^{2+} human breast cancer cell lines. 49

Figure 15. Metformin treatment suppresses PKM2 gene expression through inhibiting c-MYC expression and promoting c-MYC degradation in Her^{2+} human breast cancer cell lines 52

Figure 16. Metformin treatment improved type 2 diabetes in MMTV-ErbB2/*Lepr*$^{db/db}$ breast cancer mouse model..... 55

Figure 17. DM2 condition increases insulin levels and anti-insulin resistance treatments significantly reduce insulin levels in MMTV-ErbB2/*Lepr*$^{db/db}$ breast cancer mouse model... 56

Figure 18. Multiplex analysis for mTOR/Akt signaling pathway..... 57

Figure 19. Adipokine expression profile in MMTV-ErbB2/*Lepr*$^{db/db}$ mice 58

LIST of TABLES

Table 1—Etiologic classification of diabetes mellitus 4

Table 2. Quantitative Real-Time PCR Primer List 27

CHAPTER 1. INTRODUCTION

1.1 General background of diabetes mellitus

Diabetes mellitus, or simply diabetes, is a complex metabolic disease characterized by chronic hyperglycemia and becoming one of the most important health issues in the United States. According to the Centers for Disease Control and Prevention (CDC), diabetes affects 25.8 million Americans which are 8.3% of the U.S. population in 2011. Based on the percentage of prediabetes patients (35% of U.S. adults aged 20 years old or older and 50% of adults aged 65 years or older) in 2005-2008, the estimated number of pre-diabetic American adults ages 20 years or older is about 79 million. It is predicted that one of three man and nearly 2 of 5 women who born in the U.S. after 200 will have lifetime risk of developing diabetes (Centers for Disease Control and Prevention. National Center for Chronic Disease Prevention and Health Promotion. Diabetes at A Glance. Atlanta, 2011; Narayan et al., 2003). The chronic hyperglycemia increases the risk of long-term complications of vascular diseases including kidney failure, nontraumatic lower-limb amputations, blindness, hypertension, heart disease, stroke, and nervous system diseases in the United States.

1.1.a Categorization of diabetes mellitus

The high levels of blood glucose of diabetes are results from defects in insulin insulin production, insulin action, or both. Diabetes can be categorized into four four major types based on American Diabetes Association (2011):

Type I diabetes: This type of diabetes is primarily caused by autoimmune destruction of β-cells in the pancreas islet. The insulin production from the β-cells in the pancreas is not sufficient for glucose storage, therefore hyperglycemia. The cause of this diabetes is partly genetic predispositions, and is also related to environment. At the end stage, there is little or no insulin secretion from the β-cells and insulin is required for patient survival. This type of patients is also at higher risk to develop other autoimmune diseases.

Type II diabetes: Among all patients with diabetes, more than 90% diabetic patients are having diabetes mellitus type 2 (DM2), which is characterized by insulin resistance, and the majority of the DM2 patients are overweight and a sedentary life style (Giovannucci et al., 2010). This form of diabetes is previously defined as insulin-independent diabetes with an insulin resistance phenotype. The cause of this type of diabetes is more related with life style and Western diet.

Other specific types of diabetes: There are also other types of diabetes that were caused by other reasons, e.g. genetic mutations in β-cell function, insulin action, cystic fibrosis, and drug/chemical-induced diabetes as shown in Table 1.

Gestational diabetes mellitus: This form of diabetes is carbohydrate intolerance resulting in hyperglycemia during pregnancy. Women who develop gestational diabetes will have high risk to develop DM2.

Table 1—Etiologic classification of diabetes mellitus

(adapted from American Diabetes Association, Diabetes Care 2011, 34(S1): S62-S69)

I. Type 1 diabetes (β-cell destruction, usually leading to absolute insulin deficiency)
- A. Immune mediated
- B. Idiopathic

II. Type 2 diabetes (may range from predominantly insulin resistance with relative insulin deficiency to a predominantly secretory defect with insulin resistance)

III. Other specific types
- A. Genetic defects of β-cell function
  1. Chromosome 12, HNF-1α (MODY3)
  2. Chromosome 7, glucokinase (MODY2)
  3. Chromosome 20, HNF-4α (MODY1)
  4. Chromosome 13, insulin promoter factor-1 (IPF-1; MODY4)
  5. Chromosome 17, HNF-1β (MODY5)
  6. Chromosome 2, *NeuroD1* (MODY6)
  7. Mitochondrial DNA
- B. Genetic defects in insulin action
  1. Type A insulin resistance
  2. Leprechaunism
  3. Rabson-Mendenhall syndrome
  4. Lipoatrophic diabetes
- C. Diseases of the exocrine pancreas
  1. Pancreatitis
  2. Trauma/pancreatectomy
  3. Neoplasia
  4. Cystic fibrosis
  5. Hemochromatosis
  6. Fibrocalculous pancreatopathy
- D. Endocrinopathies
  1. Acromegaly
  2. Cushing's syndrome
  3. Glucagonoma
  4. Pheochromocytoma
  5. Hyperthyroidism
  6. Somatostatinoma
  7. Aldosteronoma
- E. Drug or chemical induced
  1. N-3-pyridylmethyl-N'-p-nitrophenylurea
  2. Pentamidine
  3. Nicotinic acid
  4. Glucocorticoids
  5. Diazoxide
  6. β-adrenergic agonists
  7. Thiazides
  8. Phenytoin
  9. γ-Interferon
- F. Infections
  1. Congenital rubella
  2. Cytomegalovirus
- G. Uncommon forms of immune-mediated diabetes
  1. "Stiff-man" syndrome
  2. Anti-insulin receptor antibodies
- H. Other genetic syndromes sometimes associated with diabetes
  1. Down syndrome
  2. Klinefelter syndrome
  3. Turner syndrome
  4. Wolfram syndrome
  5. Friedreich ataxia
  6. Huntington chorea
  7. Laurence-Moon-Biedl syndrome
  8. Myotonic dystrophy
  9. Porphyria
  10. Prader-Willi syndrome

IV. Gestational diabetes mellitus

Patients with any form of diabetes may require insulin treatment at some stage of their disease. Such use of insulin does not, of itself, classify the patient.

1.2 General background of breast cancer

Although breast cancer mortality is decreasing due to increased awareness, improved detection/screening methods, and novel treatments, it is remaining the most frequent diagnosed cancer and the second leading cause of cancer death in women. During 2014, there are estimated 232,670 new cases of invasive breast cancer and an estimated 40,000 of breast cancer death for women in the United States. The lifetime risk for women to develop breast cancer is about one in eight (American Cancer Society, 2014).

Breast cancer is now considered a heterogeneous group of diseases that have different molecular subtypes and responses to the treatments. Therefore, they need to be well categorized in order to achieve effective treatments. By taking advantage of DNA microarray technology, we could classify breast cancer gene expression profiles and cluster them into five main molecular subtypes as shown in **Figure 1**. (Herschkowitz et al., 2007; Perou et al., 2000; Prat and Perou, 2009, 2011; Vargo-Gogola and Rosen, 2007). The five molecular subtypes are: Luminal A, Luminal B, HER2, basal-like and claudin-low breast cancer. These subtypes can also be identified by using cell surface receptors as biological markers including estrogen receptors (ER+/ER-), progesterone receptors (PR+/PR-), and human epidermal growth factor receptor 2 (HER2+/HER2-) (Reis-Filho and Pusztai, 2011). By categorizing different types of breast cancer, we are able to predict the prognosis and select

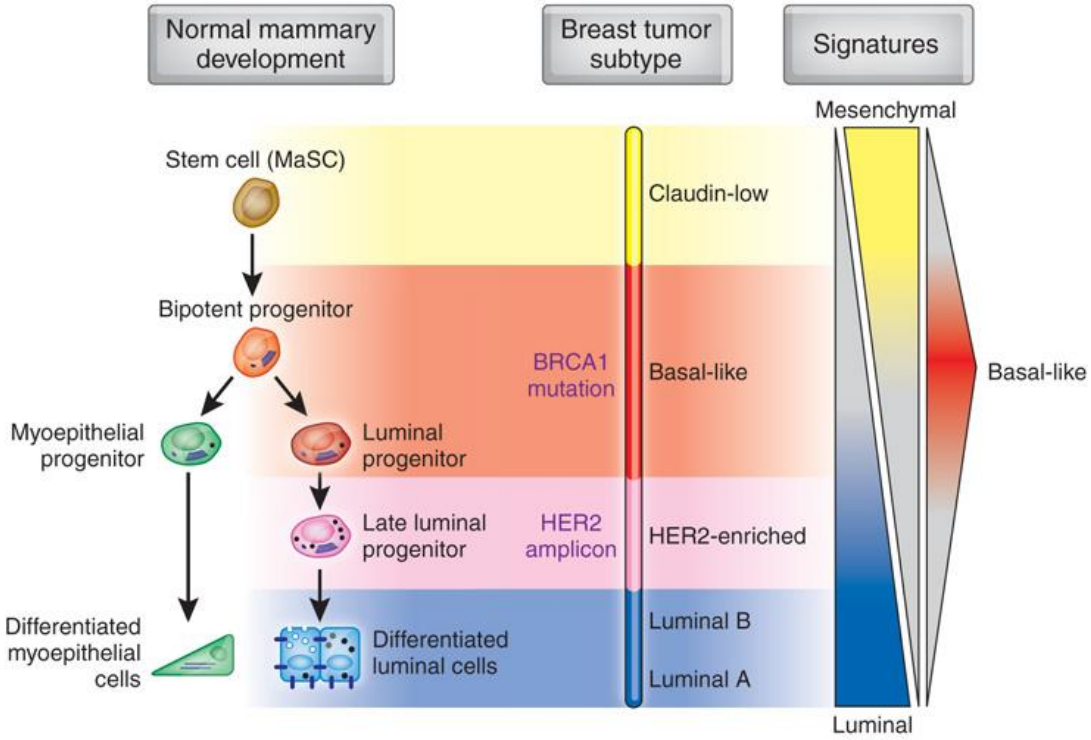

Figure 1. The five major subtypes of breast cancer and the link to normal human mammary epithelial hierarchy

Breast cancer can be categorized into five major subtypes by clustering their molecular expression patterns of normal breast tissue and breast cancer. These cancer cells may differentiate at certain stage and become one type of breast cancer. The expression pattern of Luminal, Mesenchymal, and Basal-like is more like a continuous spectrum instead of discrete discontinuous entities. Mammary stem cell (MaSC) has similar expression pattern compared to Claudin-low subtype of breast cancer. (Adapted by permission from Macmillan Publisher LtD: Nature Medicine, Part et al., Nat Med. 2009, 15(8): 842-4, Copyright 2009).

suitable treatments for breast cancer patients (Goldhirsch et al., 2011) as shown in **Figure 2**.

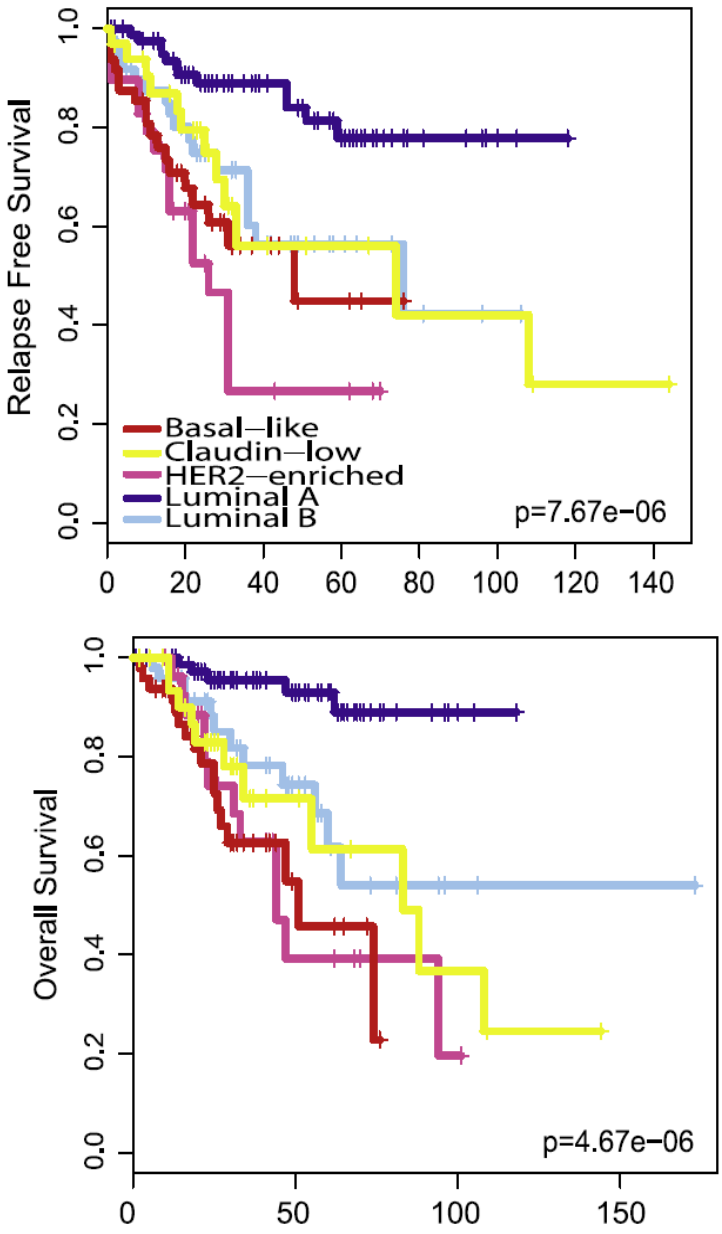

Figure 2. Patient relapse survival and overall survival on different breast cancer subtypes

Kaplan-Meier survival curves were plotted by using UNC337 data set. (Adapted by permission from Elsevier: Molecular Oncology, 5(1), Prat and Perou, Deconstructing the molecular portraits of breast cancer, 5-23, Copyright Elsevier (2011).

Luminal A breast cancer is the most common subtype representing about 40% in the breast cancer population (Perou and Borresen-Dale, 2011) and the receptor status of these tumors is ER+ and/or PR+ and HER2-. Because of the expression of ER, hormonal therapy strategies such as tomaxifen and aromatase inhibitors could be considered as treatment options for patients. In clinic, luminal A breast cancer shows low proliferation, low grade, less aggressive phenotype, and has better outcome in patient survival.

Luminal B breast cancer is ER+ and /or PR+. The HER2 status can be either HER2+ or HER2- with high Ki67 staining. The histological grade lymph node-positive rate is higher comparing to Luminal A (Voduc et al., 2010). The prognosis is not so good comparing with Luminal A breast cancer, but can use hormonal therapies as treatment options.

HER2$^+$ breast cancer accounts for 20-25% of breast cancer cases and is associated with poor prognosis with early and frequent recurrence (Piccart-Gebhart et al., 2005; Sorlie et al., 2003). Patients in this group have high level of HER2 expression with high metastasis rate and aggressive phenotype. Trastuzumab (Herceptin) treatment significantly improves patient survival (Ross et al., 2003).

Basal-like breast cancer can be clinically referred to triple negative breast cancer based on the receptor status (ER-, PR-, and HER2-) although the

molecular expression profiles can be not exactly the same. The tumors usually have high expression in basal epithelial markers (i.e. cytokeratins) and growth factor receptors (i.e. EGFR) (Sorlie et al., 2003; Sotiriou et al., 2003).

Claudin-low breast cancer is recently identified by the low expression of tight junction and cell adhesion proteins (Claudins 3, 4, 7, Occludin, and E-cadherin) (Herschkowitz et al., 2007) with ER-, PR- HER2- phenotype. The molecular expression pattern is similar to the stem cell stage compared to the normal mammary development (Prat et al., 2010). The stem-cell property might contribute the recurrence and poor prognosis in patients (Creighton et al., 2009).

There is also a group of breast cancer called normal-like breast cancer and the gene expression pattern is very close to normal breast tissue. In fact, the normal-like breast cancer samples for microarray studies have always contained normal breast tissue which might explain why this group was clustered with normal breast tissue in the gene expression profiling analysis (Prat and Perou, 2011). It needs to be further confirmed with large scale of data. In clinic, normal-like tumors are usually small and the patients usually have good prognosis (Carey et al., 2006; Fan et al., 2006).

In conclusion, the transcriptomic analyses allow us to understand the origin of breast cancer and reveal potential therapeutic targets for different types of breast cancer. Although the target therapies had been established to different types of breast cancer, many cancer patients eventually develop resistance for their treatments. On

the other hand, patients who were diagnosed with breast cancer may also under multiple chronic conditions, including diabetes. Better understanding of intervention treatments to manage breast cancer and other complications will allow us to develop new therapeutic strategies to treat breast cancer.

1.3 Diabetes treatments, insulin levels, and anti-cancer effects

Although diabetes is a serious disease, it can be managed with proper treatments. In the clinic, one of the primary goals to manage diabetes is to reduce the blood glucose level in patients. Therefore, doctors may prescribe insulin or modified insulins to diabetic patients regardless of the serum level of insulin in the patients. More insulin will increase the uptake of glucose and reduce the level of glucose in the blood in diabetic patients. There are other treatment options that involved in increase insulin levels. While sylfonylureas and glinides stimulate insulin release from the β-cells of the pancreas, glucagon-like peptide-1 (GLP-1) receptor agonists not only stimulate insulin secretion from the β–cells of the pancreas, but also inhibit glucagon release from the α-cells. Besides that, DPP-4 inhibitors increase GLP-1 and glucose-dependent insulinotropic polypeptide (GIP) by inhibiting the enzyme that degrades incretin hormones. However, the increased circulating levels of insulin is linked to a higher risk of cancer (Bowker et al., 2006; Butler, 2009; Colhoun, 2009; Hemkens et al., 2009; Monami et al., 2009).

There are also treatments that do not directly regulate insulin levels, such as α–glucosidase inhibitors and amylin agonists. While α–glucosidase inhibitors block carbohydrate digestion, amylin agonists slow down gastric emptying and inhibit glucogon production. Surprisingly, biguanides (e.g., metformin) and thiazolidinediones (e.g., rosiglitazone) are two common orally administered treatments for DM2 and have showed anti-tumor effect for multiple cancer types (Ben Sahra et al., 2008; Buzzai et al., 2007; Giovannucci et al., 2010; Girnun et al., 2007; Hirsch et al., 2013; Monami et al., 2008), including breast cancer (Zhu et al., 2011; Zhuang and Miskimins, 2008).

1.3.a Metformin

Metformin is recommended as a first line treatment for DM2 with high tolerance and low side effect. Although the usage of metformin was linked to lactic acidosis (Wiholm and Myrhed, 1993), a meta-analysis study had showed that the incidence of lactic acidosis in the metformin and non-metformin group was 8.1 and 9.9 cases per 100,000 patient-years, respectively (Salpeter et al., 2003). Another new study done by Bristol-Myers Squibb Company indicated that there is no lactic acidosis in 7,227 patients who received metformin treatment (Cryer et al., 2005).

Even though the detail mechanism of metformin action is only partially understood, the major function of metformin is to lower glucose levels and to improve insulin sensitivity. It is believed that the high levels of organic cation transporter 1 (OCT1) in the liver mediate hepatic metformin uptake (Shu et al., 2007).

Metformin improves insulin receptor sensitivity through upregulation of insulin-receptor-substrate-2 (IRS-2) in the liver. It also increases translocation of glucose transporter (GLUT)-1 (Gunton et al., 2003). At the same time, metformin inhibits hepatic gluconeogenesis (Shaw et al., 2005). It is also reported that metformin treatment increases glucose uptake in the skeletal muscle (McIntyre et al., 1991).

Metformin is also a well-known mitochondrial complex I inhibitor (Owen et al., 2000). Once the mitochondrial electron transport chain is inhibited, adenosine triphosphate (ATP) production in the cell is decreased and adenosine monophosphate (AMP)/ATP ratio is increased. The upregulated AMP may lead to the inhibition of glucagon-induced cyclic adenosine monophosphate (cAMP) synthesis (Miller et al., 2013) or AMPK activation (Fryer et al., 2002). Although it is believed that metformin activated AMPK and mediated glucose homeostasis (Zhou et al., 2001) through Liver Kinase B1 (LKB1) (Shaw et al., 2005), a recent study indicated that metformin inhibits hepatic gluconeogenesis through a LKB1/AMPK independent pathway (Foretz et al., 2010).

1.3.b Rosiglitazone

Rosiglitazone is one of the thiazolidinediones (TZDs) available for diabetic patients to control their blood glucose. TZDs are agonists of peroxisome proliferator-activated receptor γ (PPARγ) (Lehmann et al., 1995).

By administrating rosiglitazone to the patients, PPARγ receptors in the nucleus are activated in a ligand-receptor dependent fashion and increase the sensitivity of insulin by turning on downstream gene expression that involved in glucose uptake (Yki-Jarvinen, 2004).

Rosiglitazone has been associated with an increased risk of heart attack, stroke and fluid retention (Home et al., 2007; Nissen and Wolski, 2007). The U.S. Food and Drug Administration (FDA) announced to restrict the usage on patients in 2010 (Graham and Gelperin, 2010; Graham et al., 2010). However, recent results from the re-adjudication of Rosiglitazone Evaluated for Cardiovascular Outcomes and Regulation of Glycemia in Diabetes (RECORD) clinical trial showed no elevated risk of heart attack or death in patients treated with rosiglitazone comparing with other standard treatments (Mitka, 2013). Therefore, the restriction has been removed by the FDA on November 25th, 2013.

Rosiglitazone treatment showed decreased cancer risk in patients (Chang et al., 2012; Monami et al., 2014; Monami et al., 2008). From previous studies, rosiglitazone treatment induces apoptosis (Ohta et al., 2001; Zou et al., 2007), blocks cell cycle (Han et al., 2004), promotes differentiation (Bren-Mattison et al., 2005), inhibits angiogenesis (Keshamouni et al., 2005) and suppresses immune response (Bren-Mattison et al., 2008). PPARγ is also one of the upstream transcriptional regulators for PTEN (Cao et al., 2007; Lee et al., 2006; Patel et al., 2001). Increased PTEN inhibits mTOR/AKT signaling pathway which is largely involved in

tumorigenesis (Maehama and Dixon, 1998). Rosiglitazone treatment also induces AMPK activation (Fryer et al., 2002; Han and Roman, 2006) and inhibits mitochondrial oxidation independent of PPARγ signaling pathway (Brunmair et al., 2001).

1.3.c Anti-insulin resistance treatments and HER2$^+$ cancer

Our recent study suggested that these pharmacologic treatments for DM2 may reduce risk, morbidity, and mortality of breast cancer with overexpression or amplification of human epidermal growth factor receptor 2 (HER2) (He et al., 2012). Several research groups have investigated the anticancer effect of the anti-insulin resistance treatments in HER2$^+$ breast cancer *in vitro* (Feng et al., 2011; Zhuang and Miskimins, 2008) and *in vivo* (Anisimov et al., 2005a; Anisimov et al., 2005b). However, the *in vitro* experiments performed in cell lines could not reflect the interaction between cancer cells and stromal cells, and unfortunately, the *in vivo* xenograft experiments were performed in nude mice or severe combined immunodeficiency (SCID) mice that lacked an intact immune system, which is essential for cancer progression. Moreover, neither high-fat diet-induced nor drug-induced diabetes models can mimic diabetes development in patients. Similarly, a transgenic diabetic model without obese conditions (Fierz et al., 2013) also could not reflect the fact that 80% of DM2 patients are overweight or obese. Therefore, a transgenic animal model with DM2, obesity, and an intact immune system to evaluate the correlation between breast cancer and

DM2 is necessary to answer the underlying questions about how anti-insulin resistance treatments reduce cancer progression.

1.4 Gap in knowledge

Clinical studies showed that diabetes is a risk factor of breast cancer. However, there is no animal model to address the impact of DM2 on HER2+ breast cancer. Previous study showed that mice with homozygous leptin receptor point mutation (*Lepr*$^{db/db}$) did not develop oncogene-induced mammary tumors in a C57BL/6J background (Cleary et al., 2004). However, the C57BL/6J (B6) genetic background is resistant to carcinogenesis (DiGiovanni et al., 1993; Drinkwater and Ginsler, 1986; Fischer et al., 1989; Rowse et al., 1998).

To clarify this question, we decided to cross MMTV-ErbB2 mice with *Lepr*$^{db/+}$ mice to generate a diabetic HER2^{+} breast cancer mouse model in a Friend leukemia virus B (FVB) genetic background. This is the first transgenic animal in a DM2 setting with spontaneous HER2^{+} tumor development and we would like to know whether DM2 promotes breast cancer progression. Furthermore, we would like to test that this aggressiveness caused by DM2 can be attenuated by anti-insulin resistance treatments in a clinical relevant concentration. The data we collected are described in the following chapters. These results may bring attention to doctors who treat HER2^{+} breast cancer patients with diabetes about their choice of anti-diabetic medications.

CHAPTER 2. MATERIAL and METHODS

2.1 Mouse Tumor Model

MMTV-ErbB2 mice (strain name: FVB-Tg (MMTV-Erbb2) NK1Mul/J; stock number: 005038) and *Lepr*$^{db/db}$ mice (strain name: B6.BKS (D)-*Lepr*^{db}/J; stock number: 000697) were purchased from The Jackson Laboratory (Maine, USA). MMTV-ErbB2/*Lepr*$^{db/db}$ double-transgenic mice were generated by crossing male MMTV-ErbB2 mice with female *Lepr*$^{db/+}$ mice in an FVB genetic background (**Figure 3**). This is necessary because MMTV-ErbB2 female mice, although fertile, are unable to lactate, and the *Lepr*$^{db/db}$ mice were infertile. This breeding strategy resulted in the production of all three *Lepr* genotypes. The offspring were maintained with their mothers until age 21 days and then subjected to genotyping. All mouse studies were carried out under a protocol approved by The University of Texas MD Anderson Cancer Center Institutional Animal Care and Use Committee.

2.2 Genotyping, Weight Measurement, Oral Glucose Tolerance Tests and Insulin Tolerance Tests

Mouse tails were snipped at weaning, and DNA was extracted from the tail for genotyping following a standard protocol provided by The Jackson Laboratory. The mice were weighted twice each week. The weight data were separated and plotted based on different genotypes. Oral glucose tolerance

tests (OGTTs) and insulin tolerance tests (ITTs) were performed as previously described (Dezaki et al., 2004).

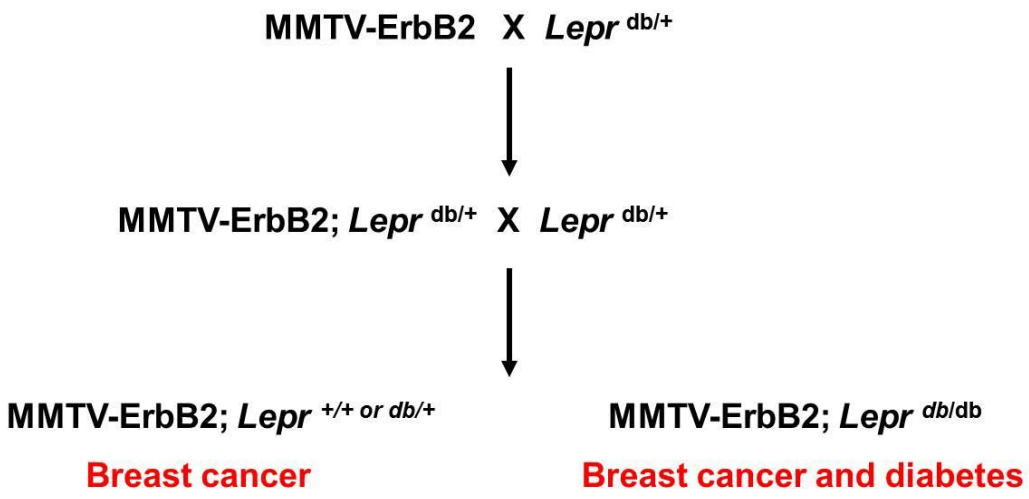

Figure 3. Scheme of mouse breading

MMTV-ErbB2 mice were crossed with *Lepr*$^{db/+}$ mice in FVB background. Genotyping were performed, and mice carring MMTV-ErbB2 gene were collected for further study.

Briefly, for OGTTs, animals were fasting overnight and 1 g/kg glucose was given to the mice via oral gavage followed by blood sampling from the tail vein for glucose measurement. For ITTs, animals were fasting for 6 hours. Insulin (1 U/kg) was intraperitoneally injected, and blood was collected from the tail vein for glucose measurement. Statistical analysis was done with GraphPad Prism for Windows.

2.3 Mammary Gland Whole-Mount Staining

Mammary gland whole-mount staining was performed following standard procedures. Briefly, mammary glands were fixed on glass slides with Carnoy's solution (glacial acetic: choloroform: ethanol, 1: 3: 6) overnight at room temperature (RT). The glands were rehydrated prior to overnight staining in aluminum carmine (1 g carmine, 2.5 g aluminum potassium sulfate boiled for 20 minutes in distilled water, filtered, and brought to a final volume of 500 mL). The glands were then stored in 70% ethanol at 4℃ overnight. Photographs were taken under a 4x power objective lens using a digital camera mounted on a Leica MZ125 microscope (Leica Instruments, Wetzlar, Germany). The tumor area was quantified using Image-Pro Plus software (MediaCybernetics, Rockville, MD, USA). Statistical analysis was done with GraphPad Prism for Windows.

2.4 Anti-diabetic Drug Treatments

For *in vivo* experiments, MMTV-ErbB2/*Lepr*$^{db/db}$ mice were treated with metformin or rosiglitazone starting at 8 weeks old. Metformin (Enzo Life Sciences, cat# 270-432-G005) was dissolved directly in distilled water (0.5 g/kg/day). Rosiglitazone (Cayman Chemical, cat# 71740) was dissolved in dimethyl sulfoxide as stock solution at 100 mM and added to distilled water (1.5 mg/kg/day). The drug treatment concentrations were within the physiologically relevant levels for diabetic patients.

For *in vitro* studies, metformin was directly dissolved in cell culture medium at desired concentrations, and 100 mM stock rosiglitazone was added into cell culture medium at desired concentrations.

2.5 Survival Analysis

Paired mice were randomly assigned to different cohorts for survival analysis. To assess the impact of diabetes on survival, we compared the survival time of MMTV-ErbB2/*Lepr*$^{db/db}$ mice (n=16) with that of MMTV-ErbB2/*Lepr*$^{db/db}$ mice (n=12). To assess the impact of anti-insulin resistance treatments on survival, we compared MMTV-ErbB2/*Lepr*$^{db/db}$ mice treated with metformin (n=14) or rosiglitazone (n=14) with MMTV-ErbB2/*Lepr*$^{db/db}$ mice without treatment (n=12). All mice were monitored weekly for tumor growth and were euthanized according to institutional protocol when tumor size reached the standard for euthanasia. Statistical analysis was done with GraphPad Prism for Windows.

2.6 Histology Staining and Mitosis Count

After the mice were euthanized, tumor samples were removed, washed in phosphate buffered saline, weighted, and fixed in 10% modified formalin. After incubation in 70% ethanol overnight, the samples were embedded in paraffin. Paraffin-embedded sections were stained with hematoxylin and eosin according to standard procedures, and mitotic cells were counted under 40x high-power fields by a pathologist.

2.7 Cell Lines and Cell Culture

Mouse cell lines were isolated from MMTV-ErbB2/*Lepr*$^{db/db}$ mice and maintained in Dulbecco's modified Eagle's medium (DMEM) with high glucose (HyClone, ref# SH30243.01) with 20% fetal bovine serum (FBS). BT-474 and MDA-MB-361 cells were gifts from Dr. Mien-Chie Hung. Briefly, cells were maintained in DMEM/high glucose supplemented with 10% FBS and cultured at 37 ℃ in 5 % CO_2 conditions.

2.8 Magnetic Resonance Spectroscopic Imaging

To determine the pyruvate/lactate conversion in mice, we collaborated with Dr. James A. Bankson in the Department of Imaging Physics at The University of Texas MD Anderson Cancer Center, and magnetic resonance spectroscopic imaging (MRSI) (Day et al., 2007; Golman et al., 2006) was

performed as described below. All experiments were performed on the same mice before and after anti-insulin resistance treatments were administered.

2.8.1 ^{13}C Polarization Process

Samples composed of 26-mg neat [1-^{13}C] pyruvic acid containing 15 mM of the trityl radical OX063 (GE Healthcare, Waukesha, WI) and 1.5 mM Prohance (Bracco Diagnostics) were polarized with dynamic nuclear polarization (DNP) at 1.4 K using a Hypersense (Oxford Instruments, Abingdon, UK) polarizer. The samples were inserted into a 3.35-Tesla vertical bore magnet and irradiated for more than 45 minutes with 94.15 GHz microwave radiation. The frozen samples were then rapidly dissolved at 180℃ in a 4 mL buffer containing 40 mM TRIS, 80 mM NaOH, and 50 mM NaCl to a final isotonic and neutral solution containing 80 mH hyperpolarized [1-^{13}C] pyruvate.

2.8.2 MRI Imaging Acquisition

All experiments were performed on a 7 T Biospec small animal MRI scanner (USR70/30, Bruker Biospin MRI, MA) equipped with BGA12 gradients (120 mm inner diameter, Gmax = 400 mT/m). A dual-tuned ^{1}H/^{13}C birdcage coil with 72-mm inner diameter (1P T10334, Bruker Biospin MRI, Inc., Ettlingen, Germany) was used for acquiring ^{1}H reference images and performing hyperpolarized ^{13}C dynamic spectroscopy. Axial and coronal slices were prescribed to contain tumors in various locations of mammary fat pads. A slice-selective pulse acquire ^{13}C sequence (TR/TE = 2000/2.4 ms, 2048 readout points, 4.96 kHz BW, 10° flip angle, 96 repetitions) was

initiated prior to ~10 s the injection of 200 µL of the hyperpolarized [1-^{13}C] pyruvate solution was performed via tail vein.

2.8.3 Data Processing

All data were processed and analyzed using custom MATLAB (The MathWorks, Inc., Natick, MA) scripts developed in our laboratory. For hyperpolarized ^{13}C experiments, data were apodized by a 15 Hz exponential window and processed by fast Fourier transform. The signal intensity from ^{13}C metabolites was calculated based on the spectral area over the full width half max, the sum of spectra over all repetitions, and the total lactate signal normalized by the sum of total pyruvate and lactate signals.

2.9 Measurement of Oxygen Consumption Rate and Extracellular Acidification Rate in Mouse mammary tumor cells from MMTV-ErbB2/*Lepr*$^{db/db}$ mice

To further determine the impact of anti-insulin resistance treatment on cancer metabolism *in vitro*, we isolated the cancer cells from tumors of the MMTV-ErbB2/*Lepr*$^{db/db}$ mice without any treatment and cultured the cells in a 24-well microplate (Seahorse Bioscience). The oxygen consumption rate (OCR) and extracellular acidification rate (ECAR) were measured via a Seahorse XF24 instrument (Seahorse Bioscience) according to the manufacturer's instructions. Briefly, mouse tumor cells were pretreated with low concentration of metformin (300 µM) and then seeded in an XF24 microplate 16 hours before the experiment. Just before the Seahorse XF assay,

the culture medium was replaced with assay medium (low-buffered DMEM containing 25 mM D-glucose, 1 mM of sodium pyruvate, and 1 mM of L-glutamine) and incubated for 1 hour at 37 ℃. After a baseline measurement of OCR and ECAR, 75 µl of mitochondrial respiratory chain inhibitors was sequentially injected into each well to reach the final working 1X concentrations. After 5 minutes of mixing to equally expose the cancer cells to the chemical inhibitors, OCR and ECAR were measured. OCR was reported in pmol/minute/mg, and ECAR was reported in mpH/minute/mg. Results were analyzed using Seahorse XF software. Statistical analysis was done with GraphPad Prism for Windows.

2.10 Proliferation assay

Human $HER2^+$ breast cancer cell lines (BT-474 and MDA-MB-361) were split in low density in 100 mm^2 dishes and cultured in DMEM/high glucose medium with 10% FBS overnight. On the second day, cells were treated with various concentrations of metformin in 10 ml of medium for 3 days. On the fifth day, the cells were treated with various concentrations of metformin in an additional 10 ml of fresh medium for another 3 days. All the supernatants and cells were collected, and cells were counted using a Z1 Coulter Particle Counter (Beckman Coulter, Brea, CA, USA). Triplicate samples were collected at each time point. Statistical analysis was done with GraphPad Prism for Windows.

2.11 Western Blot Analysis

BT-474 and MDA-MB-361 cells were treated with various concentrations of metformin or rosiglitazone for 2 days or 6 days. Standard Western blotting of whole-cell lysates was performed with antibodies for PKM2, PDK1, PARP (Cell Signaling Technologies), and c-MYC (Epitomics). β-ACTIN (Sigma) was used as a control for loading and transfer. To determine the c-MYC proteasome-dependent degradation, BT-474 cells were treated with metformin for 2 days, and 10 μM of MG132 was applied 6 hours before sample collection. Cell lysates were subjected to standard Western blotting for c-MYC. For the c-Myc ubiquitination assay, BT474 cells were treated with MG132 for 6 hours before sample collection. Cell lysates were immunoprecipitated with anti-ubiquitin antibody and, polyubiquitinated c-Myc was immunoblotted with anti-c-MYC antibody. To determine the c-MYC turnover rate, we added 500 μg/ml cycloheximide to the culture medium, and collected samples at different time points. c-MYC density was quantified using Image J software and plotted with GraphPad Prism for Windows.

2.12 Quantitative Real-Time Polymerase Chain Reaction

For quantitative real-time polymerase chain reaction (qRT-PCR), total RNA was collected from BT-474 cells using Trizol reagents (Invitrogen), and cDNA was synthesized using an iScript cDNA synthesis kit (BioRad). qRT-PCR was performed with an iQ-SYBR Green Supermix (BioRad) and an

iCycler CFX96 RT-PCR detection system (BioRad). Primer sequences were showed in Table 3. 18S rRNA was used for normalization. Statistical analysis was done with GraphPad Prism for Windows.

Table 2. Quantitative Real-Time PCR Primer List

c-MYC-Forward	5’-GCTGTAGTAATTCCAGCGAGAGACA-3
c-MYC-Reverse	5’-CTCTGCACACACGGCTCTTC-3’
PKM2-Forward	5’-CGCCCACGTGCCCCCATCATTG-3’
PKM2-Reverse	5’-CAGGGGCCTCCAGTCCAGCATTCC-3’
18S rRNA-Forward	5’-CGGCGACGACCCATTCGAAC-3’
18S rRNA-Reverse	5’-GAATCGAACCCTGATTCCCCGTC-3’

2.13 Enzyme-linked Immunosorbent Assay

Blood samples were taken from MMTV-ErbB2/*Lepr*$^{+/+}$ mice, MMTV-ErbB2/*Lepr*$^{db/db}$ mice, MMTV-ErbB2/*Lepr*$^{db/db}$ mice with metformin treatment, and MMTV-ErbB2/*Lepr*$^{db/db}$ mice with rosiglitazone treatment. Serum samples were collected by using BD Microtainer tubes with ethylenediaminetetraacetic acid EDTA (REF# 365973) and were frozen at -80 ℃. An enzyme-linked immunosorbent assay (ELISA) was performed according to the manufacturer's instructions (EMD Millipore, rat/mouse insulin 96-well plate assay, cat# EZRMI-13K, Missouri, USA). Briefly, mouse serum samples were thawed on ice, and 10 µl of sample was added to the plate. Then, 80 µl of detection antibody was added to all wells. The plate was covered with plate sealer and incubated at RT for 2 hours on an orbital microtiter plate shaker. After the plate was washed by wash buffer, 100 µl of enzyme solution was added to all wells, and the plate was incubated at RT for 30 minutes on the plate shaker. After the plate was washed again with wash buffer, 100 µl of substrate solution was added to all wells, and the plate was incubated on the shaker for 20 minutes. Then, 100 µl stop solution was added to all wells and absorbance was measure at 450 nm and 590 nm. Statistical analysis was done with GraphPad Prism for Windows.

2.14 Multiplex Assay

Tumor samples were isolated from MMTV-ErbB2/*Lepr*$^{db/db}$ mice treated with metformin, rosiglitazone, or control group and stored at -80 ℃. Fresh tumor lysates were prepared on assay day, and a multiplex assay was performed according to the manufacturer's instructions (EMD Millipore, 11-Plex Akt/mTOR Panel –

Phosphoprotein, Cat# 48-611). Briefly, tumor lysates were diluted 1:1 with MILLIPLEX $_{MAP}$ Assay Buffer 2. Bead suspension and diluted lysates were added, and the assay plate was incubated overnight at 4 ℃ on a plate shaker protected from light. On the second day after the plate was washed with wash buffer, biotinylated reporter was added to each well, and the plate was incubated for 1 hour at RT on the plate shaker and protected from light. After the reporter was removed via vacuum filtration, MILLIPLEX $_{MAP}$ streptavidin-phycoerythrin was added to each well, and the plate was incubated for 15 minutes at RT on the plate shaker and protected from light. Without removing streptavidin-phycoerythrin, we added MILLIPLEX $_{MAP}$ amplification buffer to each well; the plate was incubated for 15 minutes at RT on the plate shaker and protected from light. Finally, the buffer was removed via vacuum filtration, and the beads in each well were resuspended using MILLIPLEX $_{MAP}$ assay buffer 2. The plate was read using Luminex 200, and the data were analyzed with GraphPad Prism for Windows.

2.15 Adipokine Array Analysis

Serum samples were prepared as previously described for the ELISA. An adipokine array assay was performed according to the manufacturer's instructions (R&D Systems, mouse adipokine array, Cat# ARY013). Briefly, membranes were blocked for 1 hour on a rocking platform. Three serum samples from each group of mice were premixed together and a detection antibody cocktail was added to serum samples following 1 hour of incubation at RT. After the blocking solution was removed, the sample-antibody mixtures were added to the membranes, and the

membranes were incubated overnight at 4 ℃ on a rocking platform. After the membranes were washed with wash buffer, membranes were incubated with streptavidin-HRP solution for 30 minutes and subjected to X-ray film exposure.

2.16 Graphs and Statistical Analysis

The log-rank test was used to determine the statistical significance of survival analysis. An unpaired t-test with Welch's correction was performed when comparing 2 groups. One-way analysis of variance followed by Bonferroni's multiple comparisons test was performed when comparing 3 or more groups. All tests were performed using GraphPad Prism version 6.0 for Windows (GraphPad Software, LaJolla, CA, USA, www.graphpad.com). Results are expressed as means ± 95% confidence interval (CI). $P < 0.05$ was considered statistically significant.

CHAPTER 3. RESULTS

3.1 Generating MMTV-ErbB2/*Lepr*$^{db/db}$ transgenic mouse model

Previous studies had shown that diabetes inhibits mammary gland development therefore inhibits tumorigenesis in transgenic mouse model (Cleary et al., 2004; Zheng et al., 2011). However, the tumor resistance B6 genetic background may life span of the MMTV-drived transgenes is longer than the *Lepr*$^{db/db}$ mice. The mice eventually died due to diabetes or obesity before breast cancer development. To verify previous findings, we generated our diabetic HER2^{+} breast cancer mouse model as shown in Figure 3.

Mice were backcrossed into an FVB genetic background, and DM2 was validated via OGTTs (Figure 4A and 4B) and ITTs (Figure 4C and 4D). Compared with the blood glucose levels in the MMTV-ErbB2/*Lepr*$^{+/+ \text{ or } db/+}$ mice, blood glucose remained high in the MMTV-ErbB2/*Lepr*$^{db/db}$ mice, indicating that the latter group developed diabetes. The body weight of MMTV-ErbB2/*Lepr*$^{db/db}$ mice was significantly greater than that of their control MMTV-ErbB2/*Lepr*$^{+/+}$ littermates (Figure 4E).

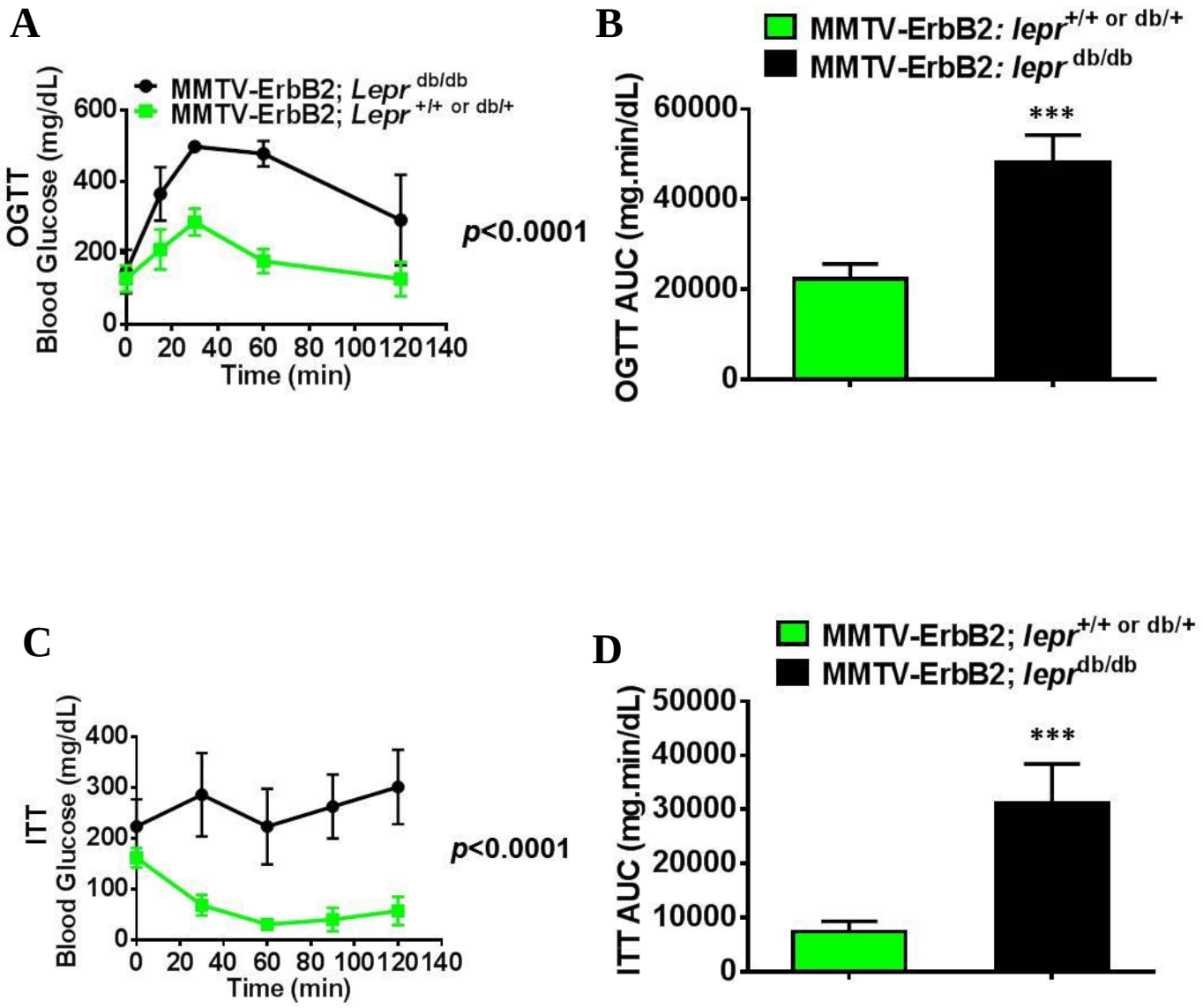
A
OGTT
Blood Glucose (mg/dL)
MMTV-ErbB2; Lepr db/db
MMTV-ErbB2; Lepr +/+ or db/+
600
400
200
0
0 20 40 60 80 100 120 140
Time (min)
p<0.0001
B
MMTV-ErbB2: lepr +/+ or db/+
MMTV-ErbB2: lepr db/db
OGTT AUC (mg.min/dL)
60000
40000
20000
0
***
C
ITT
Blood Glucose (mg/dL)
400
300
200
100
0
0 20 40 60 80 100 120 140
Time (min)
p<0.0001
D
MMTV-ErbB2; lepr +/+ or db/+
MMTV-ErbB2; lepr db/db
ITT AUC (mg.min/dL)
50000
40000
30000
20000
10000
0
***

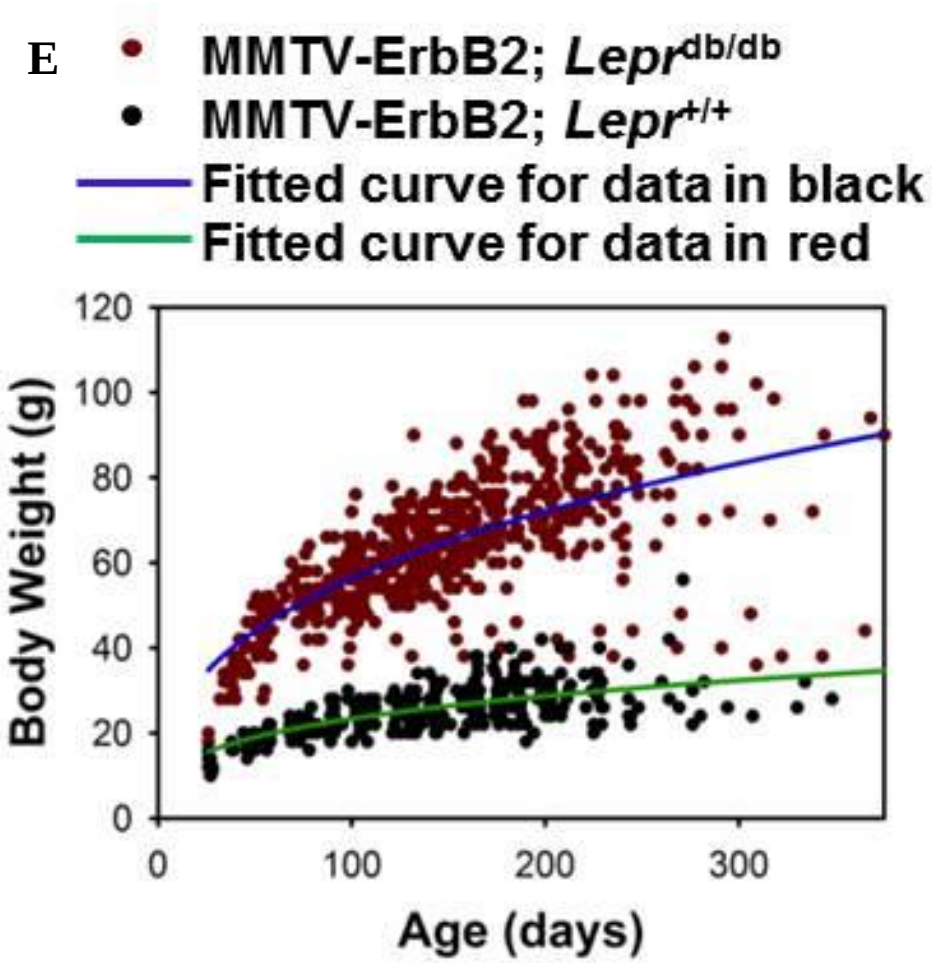

Figure 4. MMTV-ErbB2; *Lepr*$^{db/db}$ mice have insulin resistance and obesity phenotype

A) Oral glucose tolerance test (OGTT) and **C)** Insulin tolerance test (ITT) were performed on MMTV-ErbB2/*Lepr*$^{+/+}$ mice (n=6) and MMTV-ErbB2/*Lepr*$^{db/db}$ mice (n=5). Area under the curve for **B)** OGTT and **D)** ITT were plotted to show the significance. Values are means ± 95% confident interval (CI). **E)** Mouse body weight change for the MMTV-ErbB2/*Lepr*$^{+/+}$ mice versus MMTV-ErbB2/*Lepr*$^{db/db}$ mice.

3.1 Diabetes promotes breast cancer progression and reduces overall survival in the MMTV-ErbB2/*Lepr*$^{db/db}$ transgenic mouse model

Next, we sought to determine the impact of diabetes on breast cancer progression. Paired mice were dissected at the same age, and mammary glands were isolated and subjected to whole-mount staining. The tumor volume was significantly greater ($P < 0.01$) in the MMTV-ErbB2/*Lepr*$^{db/db}$ mice than in the MMTV-ErbB2/*Lepr*$^{+/+}$ mice (Figure 5A and 5B). In addition, the MMTV-ErbB2/*Lepr*$^{db/db}$ mice died at a significantly younger age than MMTV-ErbB2/*Lepr*$^{+/+}$ mice (Figure 6A, $P = 0.0004$). The median survival duration for the MMTV-ErbB2/*Lepr*$^{db/db}$ and MMTV-ErbB2/*Lepr*$^{+/+}$ mice was 5.9 months and 7.6 months, respectively. Tumor-free survival was also dramatically shorter in the MMTV-ErbB2/*Lepr*$^{db/db}$ than in the MMTV-ErbB2/*Lepr*$^{+/+}$ mice (Figure 6B, $P < 0.0001$). The median tumor-free survival duration for the MMTV-ErbB2/*Lepr*$^{db/db}$ and MMTV-ErbB2/*Lepr*$^{+/+}$ mice was 5.3 months and 6.7 months, respectively. These data indicate that DM2 group has a poorer outcome than the non-DM2 group in the HER2^{+} breast cancer mouse model.

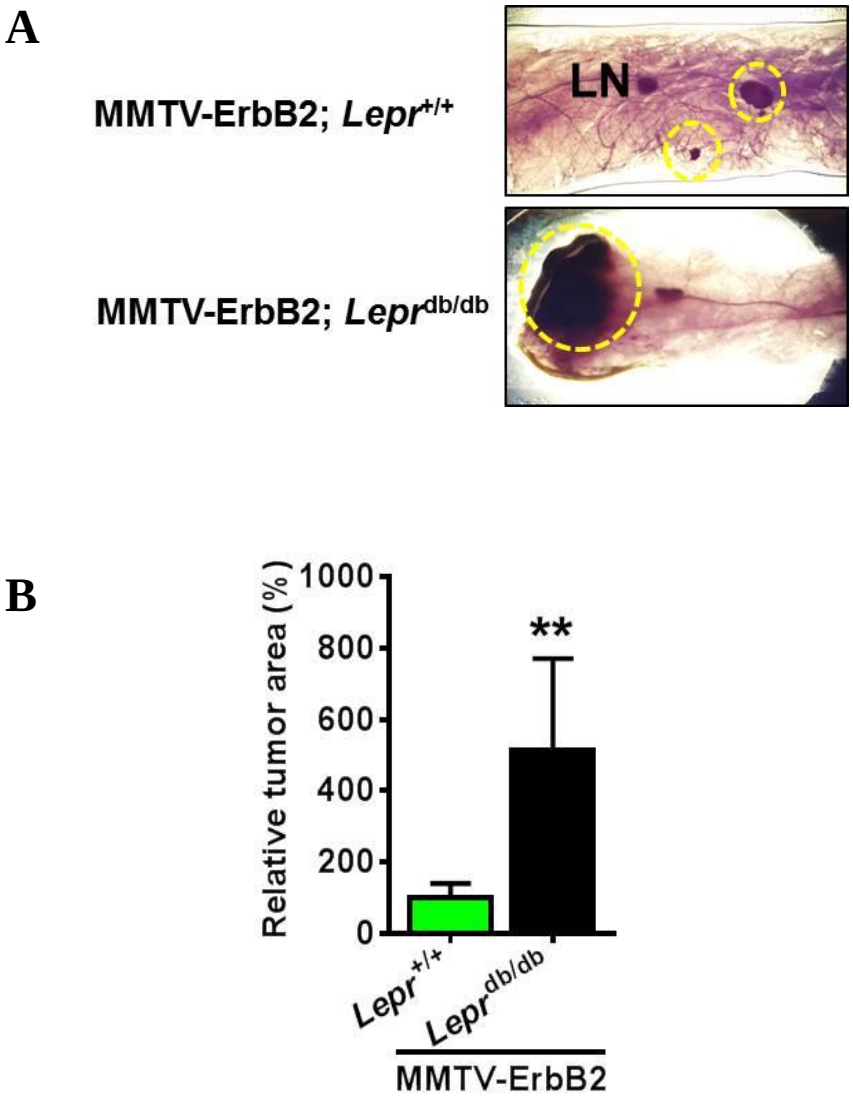

Figure 5. DM2 promotes breast cancer progression in MMTV-ErbB2; *Lepr*$^{db/db}$ mouse model

A) Representative mammary whole mount staining for the MMTV-ErbB2/*Lepr*$^{+/+}$ mice versus MMTV-ErbB2/*Lepr*$^{db/db}$ mice. Tumor area was circled in yellow. LN= lymph node. **B)** Quantitative analysis of A). Pictures were taken under dissection microscope and quantified by Image-Pro software. Values are means ± 95% CI. Mouse number: MMTV-ErbB2/*Lepr*$^{+/+}$=13; MMTV-ErbB2/*Lepr*$^{db/db}$=12.

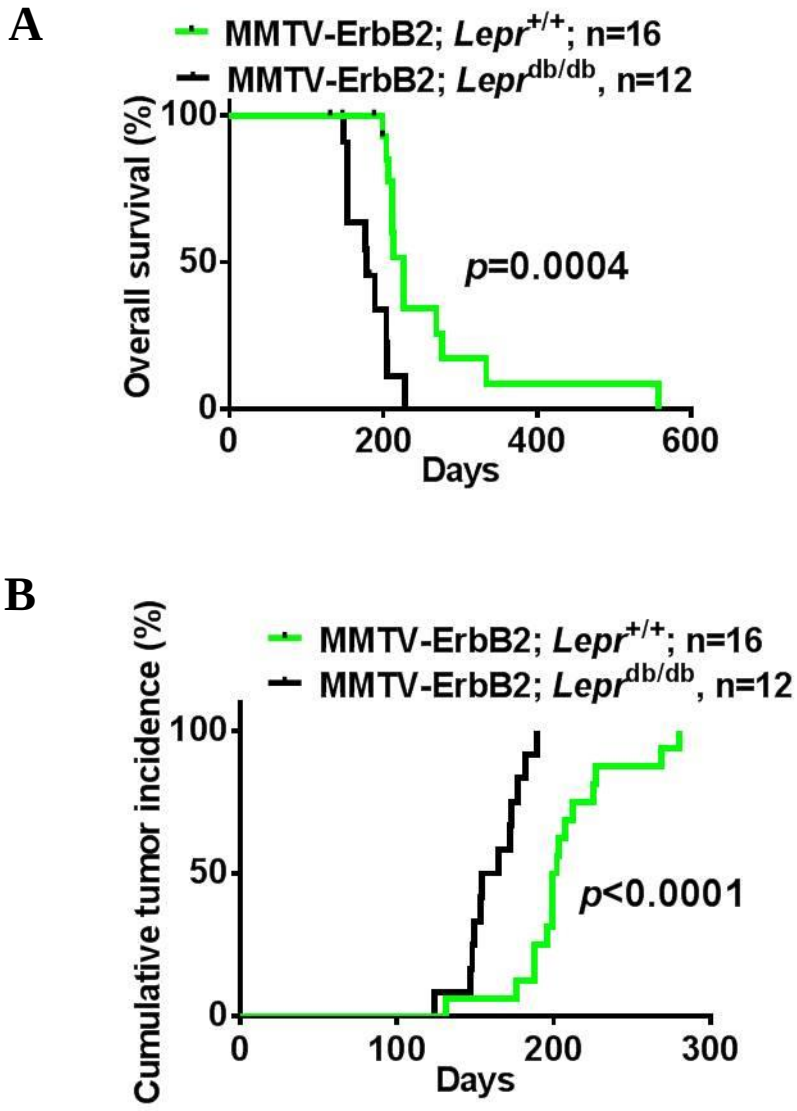

Figure 6. DM2 reduces overall survival and tumor-free survival in MMTV-ErbB2; *Lepr*$^{db/db}$ mouse model

A) Overall survival and **B)** Cumulative tumor incidence for MMTV-ErbB2/*Lepr*$^{+/+}$ mice (n=16) versus MMTV-ErbB2/*Lepr*$^{db/db}$ mice (n=12). The log-rank test was used to determine the statistical significance of survival analysis.

3.2 Anti-insulin resistance treatments attenuate tumor progression and improve overall survival in HER2^{+} breast cancer diabetic mouse model

MMTV-ErbB2/*Lepr*$^{db/db}$ mice were assigned to one of three groups: non-treatment control, metformin treatment, or rosiglitazone treatment. The treatments prolonged overall survival (Figure 7A) and tumor-free survival (Figure 7B) in the mouse model. Mammary glands were isolated from mice of similar ages and then subjected to whole-mount staining. Whole-mount staining showed that anti-insulin resistance treatments inhibited tumor progression in the mammary glands (Figure 8A) and significantly reduced the tumor size (Figure 8B, $P < 0.0001$). Ductal carcinoma *in situ* was found in the mammary fat pad paraffin sections from mice treated with metformin, indicating that metformin treatment postponed breast cancer progression in MMTV-ErbB2/*Lepr*$^{db/db}$ mice (Figure 9). Histology analysis showed that tumor samples from MMTV-ErbB2/*Lepr*$^{db/db}$ mice were poorly differentiated with solid growth patterns, high nuclear grades, and high mitotic counts. Compared with control samples, the anti-insulin resistance treatment groups were moderately differentiated with glandular formation and lower mitotic counts (Figure 10). Drug treatments extented overall survival, delayed tumor onset, and reduced cancer aggressiveness in our diabetic HER2^{+} breast cancer mouse model.

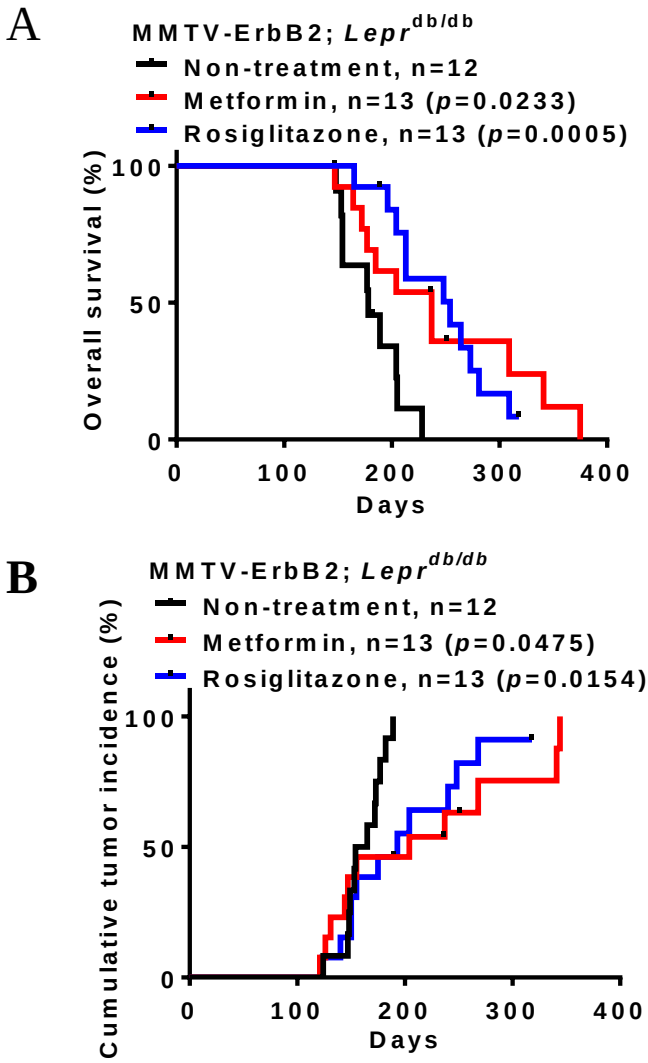

Figure 7. Anti-insulin resistance treatments improve overall survival and tumor-free survival in MMTV-ErbB2; *Lepr*$^{db/db}$ mouse model

A) Overall survival time for MMTV-ErbB2/*Lepr*$^{db/db}$ mice treated with control (n=12), metformin (n=13), and rosiglitazone (n=13). **B)** Cumulative tumor incidence rate for MMTV-ErbB2/*Lepr*$^{db/db}$ mice in different treatment groups. The log-rank test was used to determine the statistical significance of survival analysis.

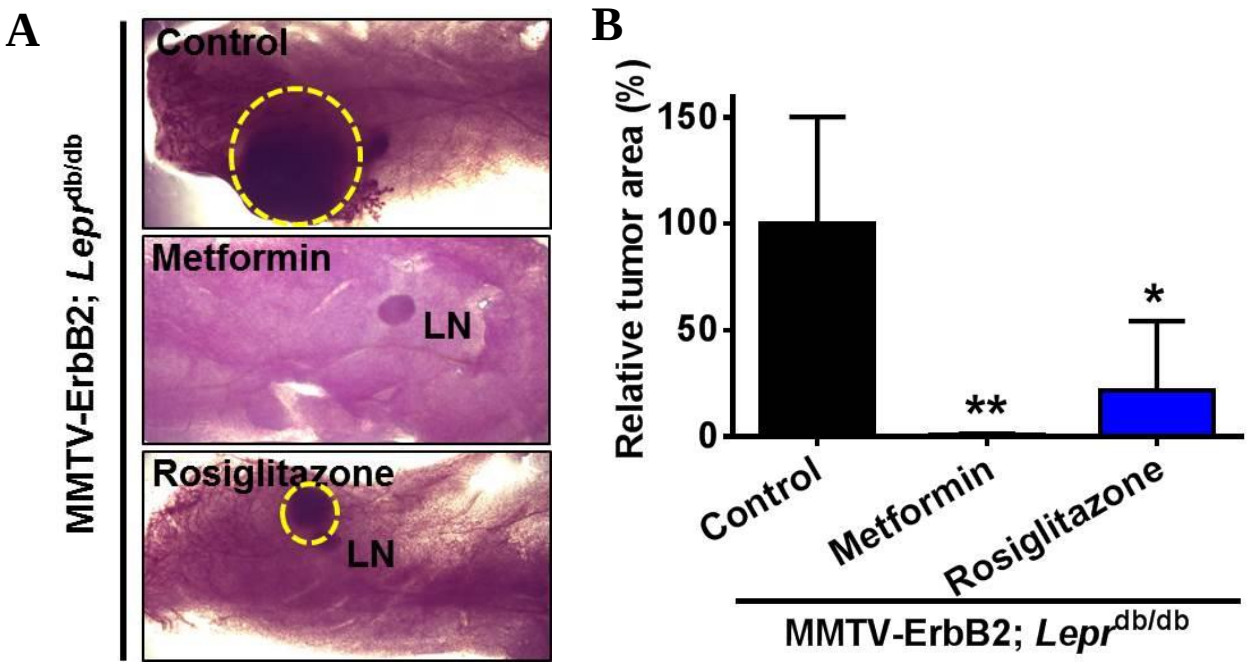

Figure 8. Anti-insulin resistance treatments attenuate tumor progression in MMTV-ErbB2/*Lepr*$^{db/db}$ mice

A) Representative mammary whole mount staining for the MMTV-ErbB2/*Lepr*$^{db/db}$ mice in different treatment groups. **B)** Quantitative bar graph represents of tumor size from C). Values are means ± 95% CI. Mouse number: control=12; metformin=6; rosiglitazone=6.

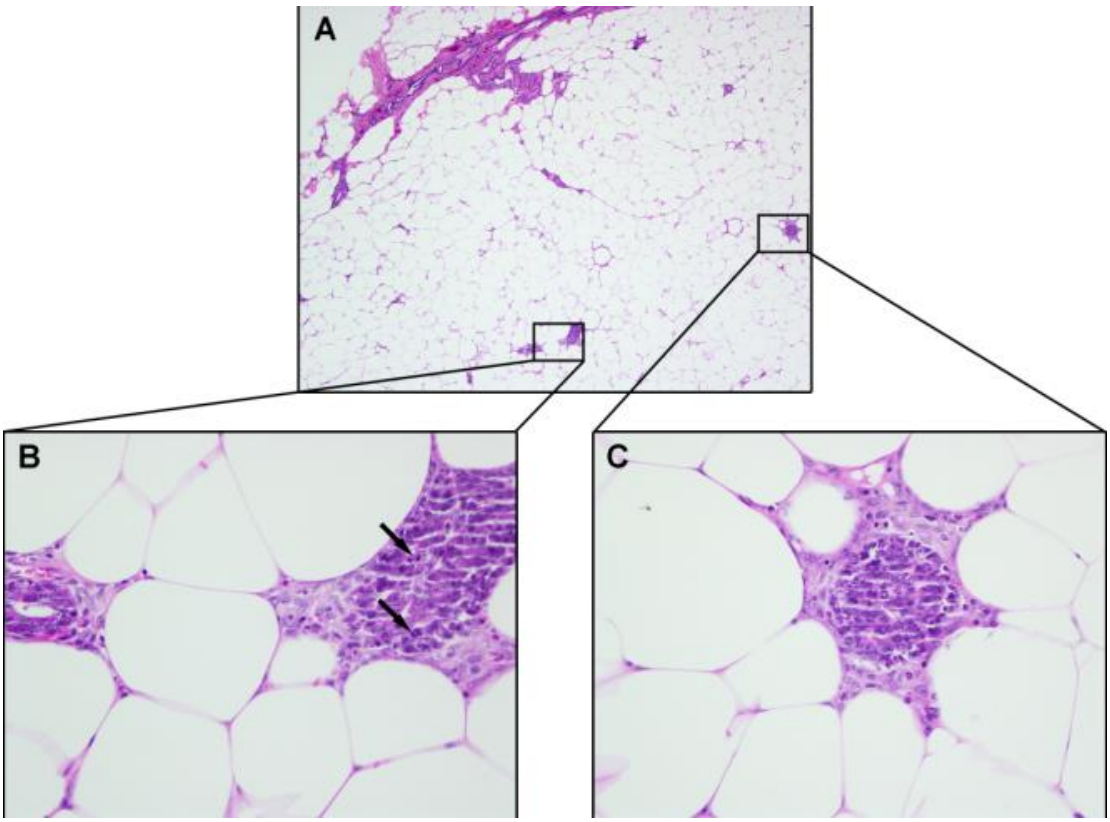

Figure 9. Metformin treatments delays tumor progression in MMTV-ErbB2/*Lepr*$^{db/db}$ mice

A) Mammary fat pads were collected from metformin treatment mice and H&E staining was performed on paraffin sections. A low power view (20X) shows two microscopic foci of dauctal carcinoma *in situ* (DCIS). **B)** and **C)** Enlarged view of two foci of DCIS, which shows enlarged ducts with solid proliferation of polymorphic tumor cells with high nuclear and cytoplasmic ratio. Arrow points mitotic figure.

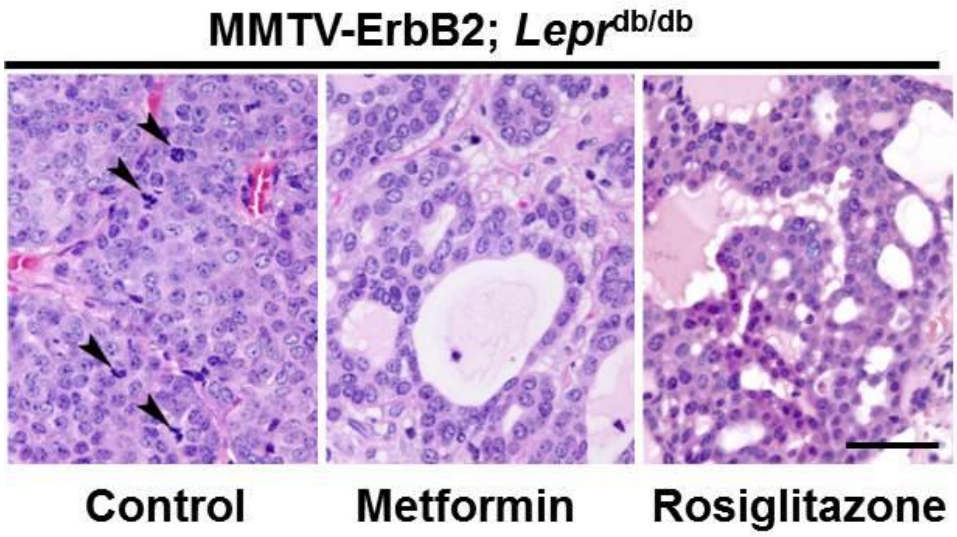

Figure 10. Anti-insulin resistant treatments repress cancer progression in MMTV-ErbB2/*Lepr*$^{db/db}$ mice.

Tumor samples were harvested from different treatment groups and H&E staining was performed on paraffin sections. Pictures were taken under 40X and pathology analysis was done by pathologist. Arrow: mitosis. Scale bar: 100 μm.

3.3 Anti-insulin resistance treatments reduce the cancer metabolism *in vivo*

To determine whether anti-insulin resistance treatments change the dynamics of the metabolic processes in MMTV-ErbB2/*Lepr*$^{db/db}$ mice, we performed MRSI to monitor the dynamic flux of pyruvate into lactate, which is the end product of aerobic glycolysis and an important marker for cancer metabolism. MRI was performed before the substrate [1-^{13}C] pyruvate injection, and the tumor area was located (Figure 11). By taking advantage of hyperpolarized technology, we injected the substrate [1-^{13}C] pyruvate into MMTB-ErbB2/*Lepr*$^{db/db}$ mice and traced the [1-^{13}C] signal to lactate *in vivo* (Figure 12A and 12B). Metformin treatment for 2 weeks caused about an 80% reduction in pyruvate/lactate conversion (Figure 12A and 12C), and 2 days of rosiglitazone treatment showed about a 50% reduction (Figure 12B and 12C). These data indicate that anti-insulin resistance treatments reduce pyruvate/lactate conversion and alter cancer metabolism *in vivo*.

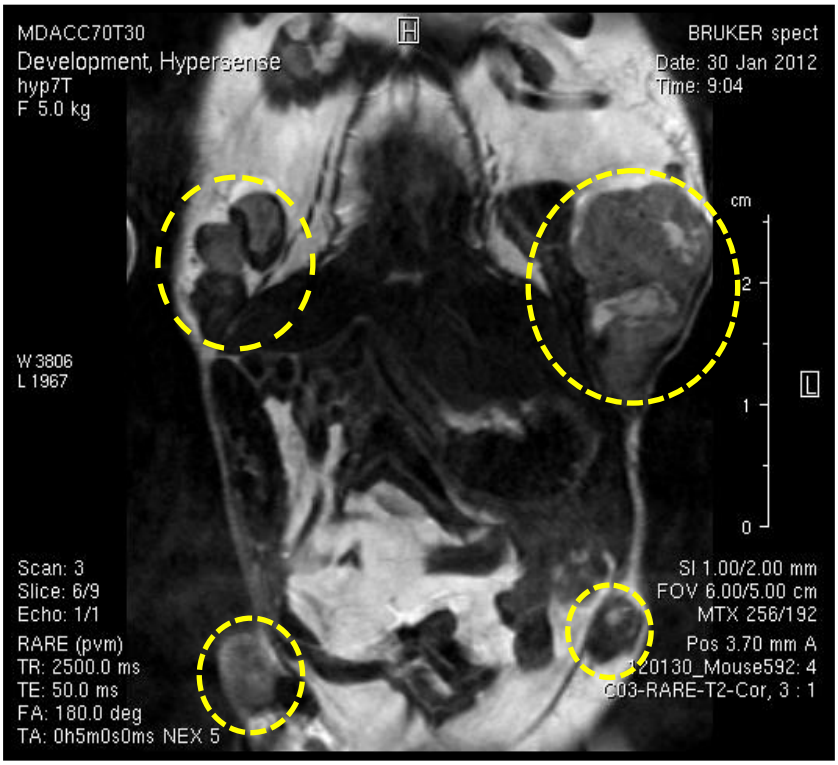

Figure 11. MRI image of tumor localization in a MMTV-ErbB2/*Lepr*$^{db/db}$ mouse

Representative T2-weighted magnetic resonance imaging (MRI) for localization of the tumor in a living MMTV-ErbB2/*Lepr*$^{db/db}$ mouse before hyperpolarized ^{13}C-pyruvate injection.

A

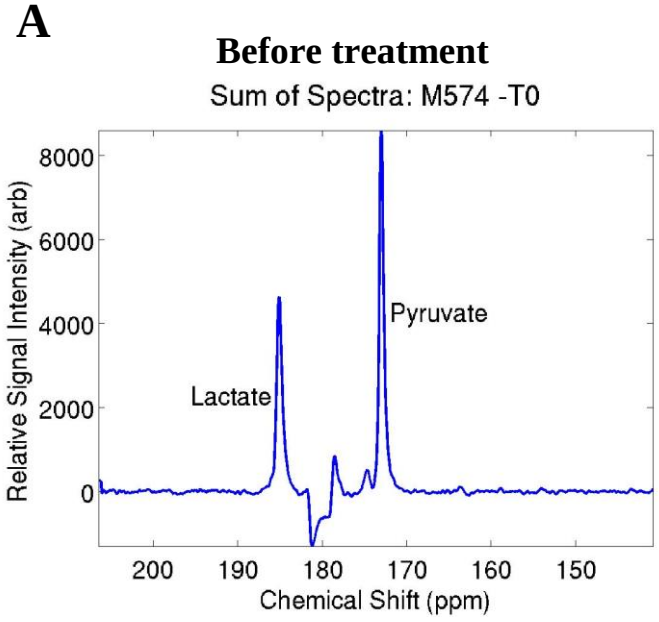
Before treatment
Sum of Spectra: M574 -T0
Relative Signal Intensity (arb)
8000
6000
4000
2000
0
Lactate
Pyruvate
200
190
180
170
160
150
Chemical Shift (ppm)

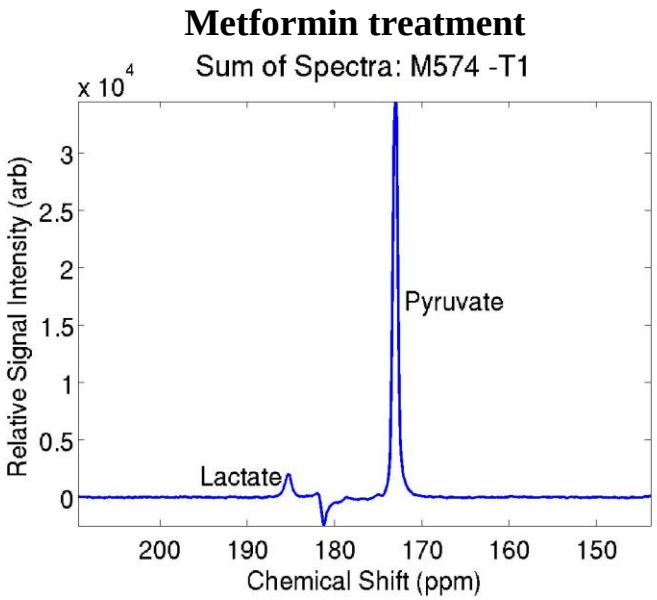
Metformin treatment
Sum of Spectra: M574 -T1
x 10^4
Relative Signal Intensity (arb)
3
2.5
2
1.5
1
0.5
0
Lactate
Pyruvate
200
190
180
170
160
150
Chemical Shift (ppm)

B

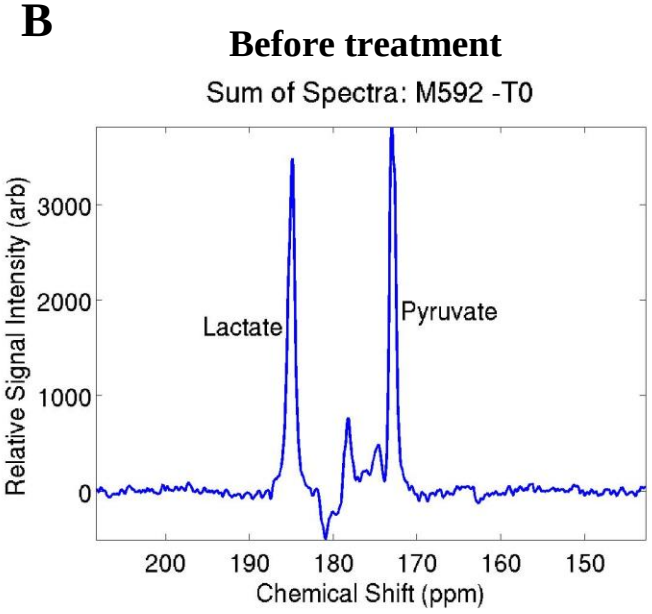
Before treatment
Sum of Spectra: M592 -T0
Relative Signal Intensity (arb)
3000
2000
1000
0
Lactate
Pyruvate
200
190
180
170
160
150
Chemical Shift (ppm)

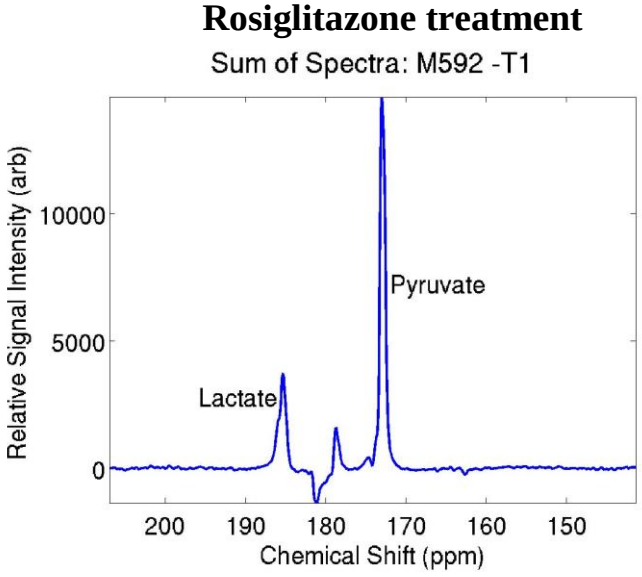
Rosiglitazone treatment
Sum of Spectra: M592 -T1
Relative Signal Intensity (arb)
10000
5000
0
Lactate
Pyruvate
200
190
180
170
160
150
Chemical Shift (ppm)

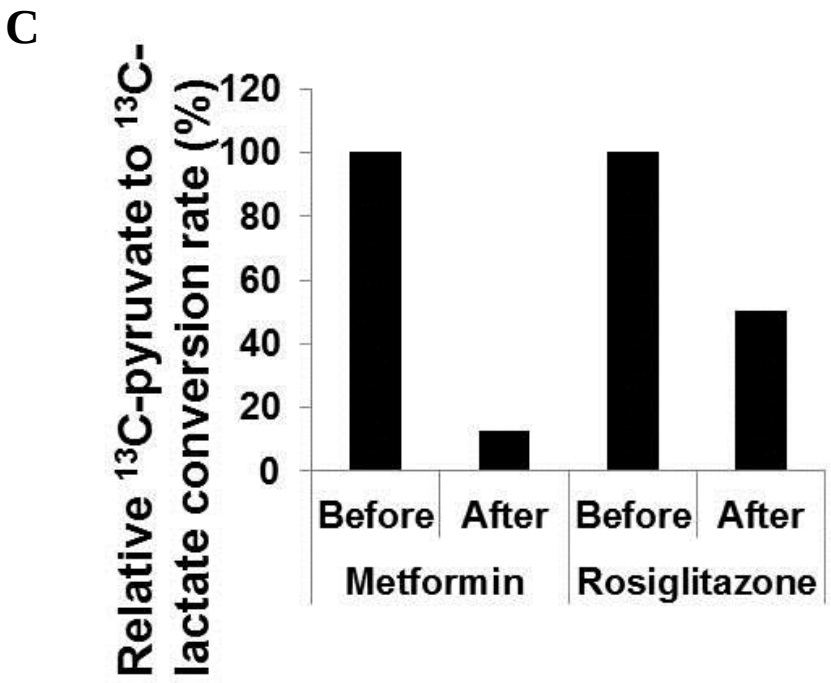

Figure 12. Anti-insulin resistant treatments reduce cancer metabolism in vivo and in vitro

A) Magnetic resonance spectroscopic imaging (MRSI) was performed on MMTV-ErbB2/*Lepr*$^{db/db}$ mice. Chemical shift after hyperpolarized ^{13}C-pyruvate was injected into MMTV-ErbB2/*Lepr*$^{db/db}$ mice before (left) or after (right) metformin treatment and **B)** rosiglitazone treatment. **C)** Quantitative bar graph represents the lactate/pyruvate conversion in tumor from A) and B)

3.4 Metformin treatment reduces mitochondrial respiration capacity and glycolysis *in vitro*

To further evaluate the impact of metformin treatment on cancer metabolism, we isolated cancer cells from the primary tumors of MMTB-ErbB2/*Lepr*$^{db/db}$ mice and seeded them into a Seahorse microplate. OCR and ECAR were measured using the Seahorse instrument. OCR was significantly lower in cells treated with 300 μM metformin than in non-treated cells (Figure 13A), indicating that mitochondrial respiration capacity was altered. Decreased ECAR also indicated that lactate production was attenuated, which confirms that glycolysis was reduced by metformin treatment (Figure 13B), as we observed in the MRSI experiment *in vivo*. These data suggest that mitochondrial respiration and both anaerobic and aerobic glycolysis were reduced upon metformin treatment. Statistical analysis of the area under the curve for OCR and ECAR revealed a significant reduction after metformin treatment (Figure 13C).

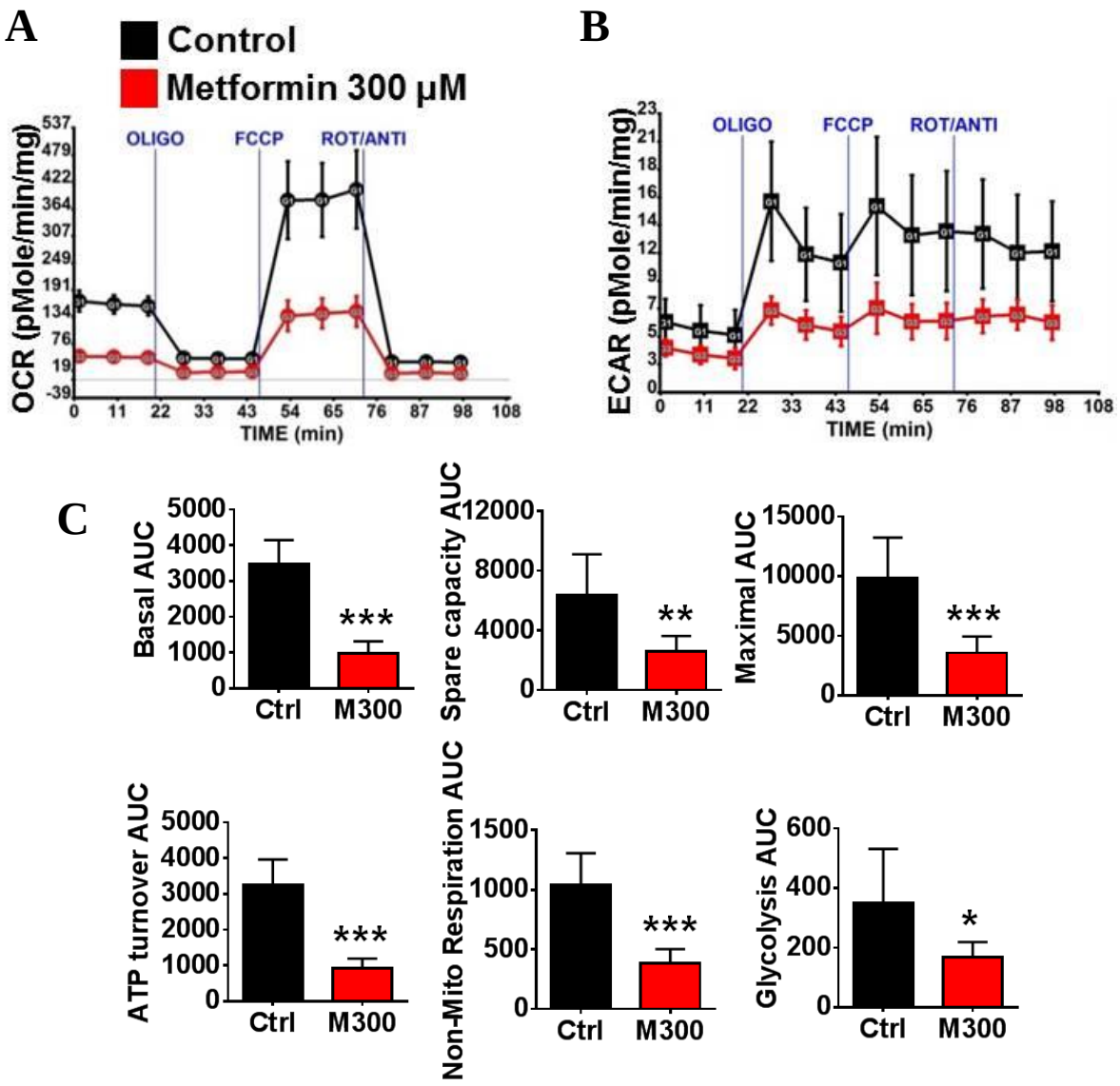

Figure 13. Metformin treatment reduces oxygen consumption (OCR) and extra cellular acidification rate (ECAR) in vitro

A) OCR and **B)** ECAR were measured by Seahorse analyzer. Tumor cells were harvested from MMTV-ErbB2/*Lepr*$^{db/db}$ mice without any treatment and seeded into 96-well plate for Seahorse analysis. Values are means ± standard deviation. **C)** Quantitative analysis of OCAR and ECAR from A) and B). Values are means ± 95% CI.

3.5 Metformin treatment inhibits proliferation, induces apoptosis, and suppresses cancer metabolism in human HER2$^+$ breast cancer cell lines

To determine whether metformin treatment also represses cancer progression and cancer metabolism in human HER2$^+$ breast cancer cells, we conducted the following experiments using BT-474 and MDA-MB-361 cells. We first split the cells at low density in 100 mm^2 dishes and treated the cells with metformin at various concentrations for 6 days. To ensure the minimum loss of dead or detached cells, we applied an additional 10 ml of medium and metformin without removing any culture medium. All supernatant and cells were collected, and the cells were quantified via a Z1 Coulter Particle Counter. In fact, metformin treatment efficiently inhibited cell proliferation (one-way analysis of variance, P<0.001, Figure 14A and 14B) started from 500 μM and induced apoptosis at 2000 μM (Figure 14C).

From the previous experiments (Figure 12 and 13), we learned that anti-insulin resistance treatments reduced cancer metabolism in vivo and in vitro. We therefore sought to determine the target of metformin treatment in human HER2+ breast cancer cell lines. c-MYC is a major player in cancer metabolism by controlling many enzymes in the glycolysis pathway at the transcriptional level. We sought to determine whether metformin treatment is involved in regulating c-MYC expression. Indeed, Western blotting showed that c-MYC expression was suppressed by metformin treatment (Figure 14C).

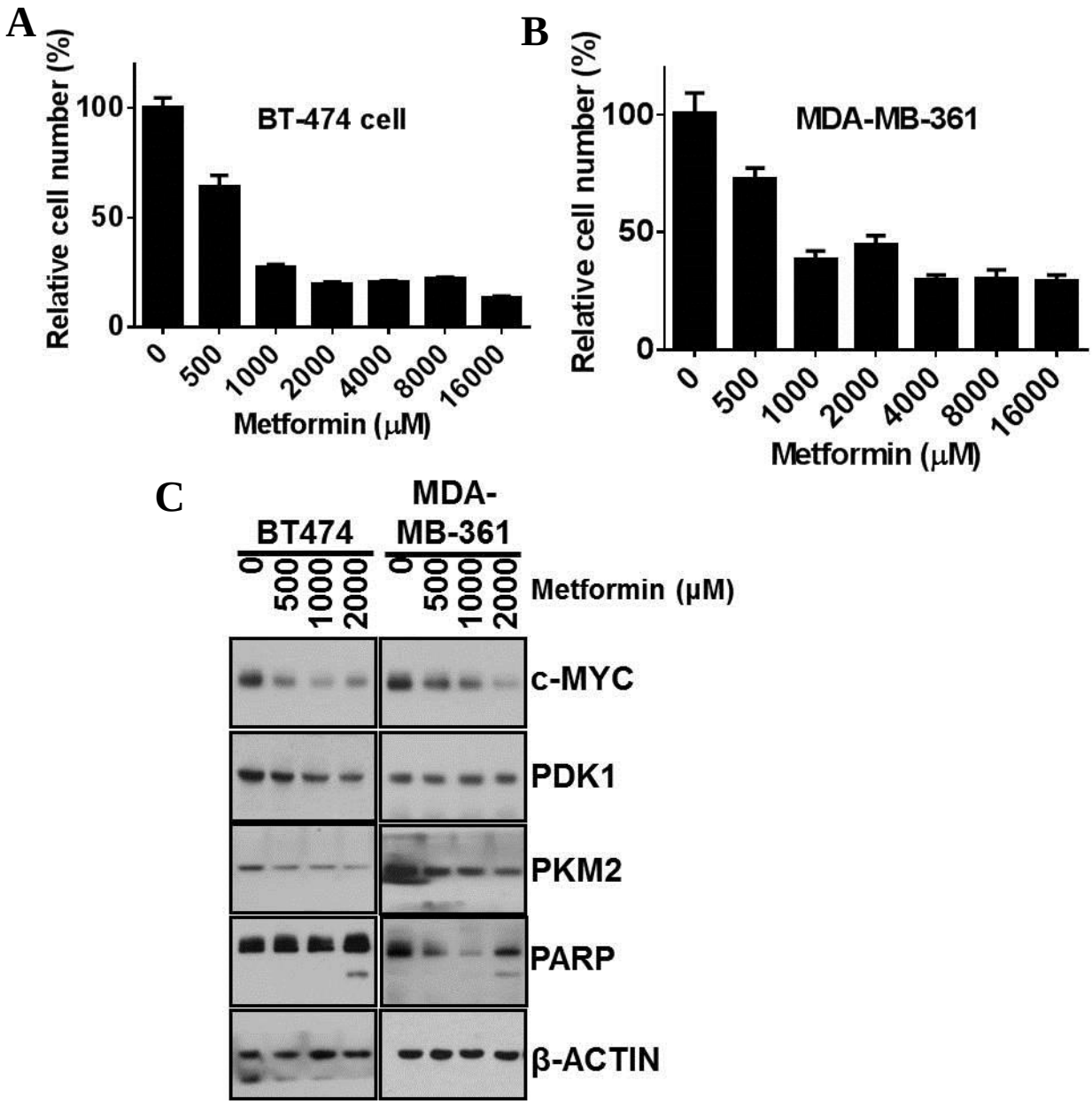

Figure 14. Metformin treatment inhibits cell proliferation, increases apoptosis, and suppresses key metabolism regulators in Her^{2+} human breast cancer cell lines.

A) BT-474 and **B)** MDA-MB-361 cell proliferation after 6 day metformin treatment at various concentrations. **C)** Western blot analysis of key metabolic protein expression and PARP cleavage after 6 days metformin treatment.

In addition, PKM2, the key step enzyme for pyruvate/lactate conversion also controlled by c-MYC, was downregulated by metformin treatment (Figure 14C). These data provide the link between the reductions in c-MYC, PKM2, and lactate production that we observed *in vivo* (Figure 12) and *in vitro* (Figure 13). We also performed qRT-PCR in BT-474 cells to determine the mRNA expression level of c-MYC and its downstream targets. Our data indicated that both c-MYC and PKM2 were downregulated at the transcriptional level in the presence of 500 μM metformin treatment (Figure 15A). After 2 days of metformin treatment, the c-MYC protein level was restored to a level comparable to that of the control in the presence of MG132, indicating that metformin treatment has a secondary mechanism of proteasome-dependent degradation (Figure 15B). A band at high molecular weight was found in the stacking gel of the ubiquitination assay, suggesting that c-MYC was highly ubiquitinated and degraded upon 2 days of metformin treatment (Figure 4F). The c-MYC protein turnover rate was also greater than that of the control (Figure 4G). Collectively, our results show that metformin treatment at clinical relevant concentrations regulates cell metabolism by downregulating c-MYC at both transcriptional and post-translational levels.

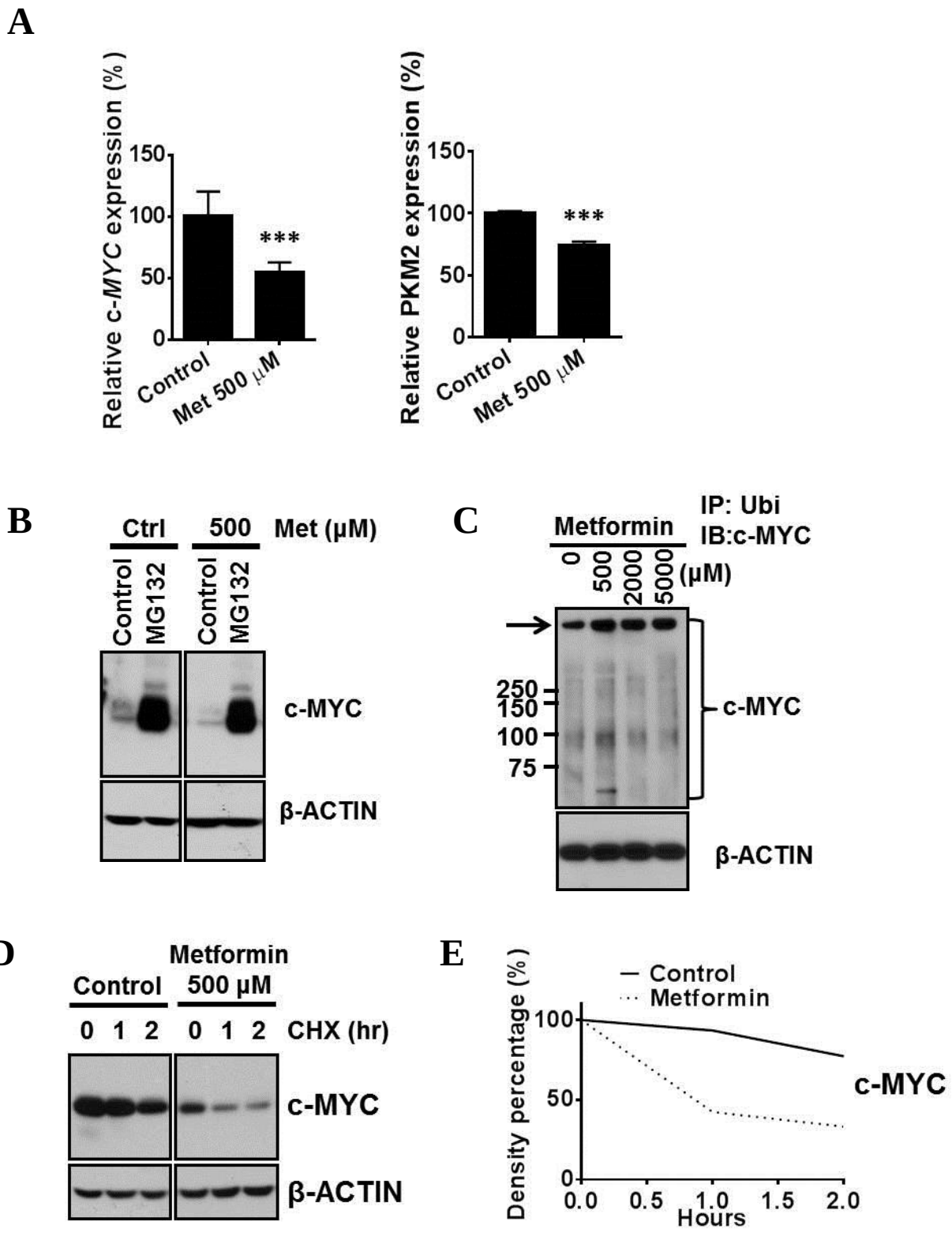
A
Relative c-MYC expression (%)
150
100
50
0
***
Control
Met 500 μM
Relative PKM2 expression (%)
150
100
50
0
***
Control
Met 500 μM
B
Ctrl
500
Met (μM)
Control
MG132
Control
MG132
c-MYC
β-ACTIN
C
Metformin
IP: Ubi
IB:c-MYC
0
500
2000
5000
(μM)
250
150
100
75
c-MYC
β-ACTIN
D
Metformin
Control
500 μM
0 1 2 0 1 2 CHX (hr)
c-MYC
β-ACTIN
E
Control
Metformin
Density percentage (%)
100
50
0
0.0 0.5 1.0 1.5 2.0
Hours
c-MYC

Figure 15. Metformin treatment suppresses PKM2 gene expression through inhibiting c-MYC expression and promoting c-MYC degradation in Her^{2+} human breast cancer cell lines

A) Real-Time PCR analysis of c-MYC (left) and PKM2 (right) mRNA expression in BT-474 cells after 2 days metformin treatment at various concentration. **B)** BT-474 cells were pretreated with metformin for 2 days and cell lysates were collected after 6 hours MG132 treatment. c-MYC protein level were shown in western blot. **C)** BT474 cells were treated with MG132 for 6 hours before harvesting. Cell lysates were immunoprecipitated with anti-ubiquitin antibody and polyubiquitinated c-Myc was immunoblotted with anti-c-MYC antibody. Arrow indicated highly ubiquitinated c-MYC at stacking gel. **D)** BT-474 cells were pretreated with metformin for 2 days and cell lysates were collected after cycloheximide (CHX) treatment at various time points. Western bolt represented the c-MYC protein level. **E)** c-MYC protein turnover. Quantitative analysis for c-MYC protein from the upper panel. Density was set as 100% at zero time point in each group.

3.6 Anti-insulin resistance treatments reduce systemic insulin level, suppress mTOR/AKT signaling in tumor, and regulate adipokine secretion profiles

From our aforementioned results, we learned that metformin treatment can efficiently suppress mitochondrial respiration, lactate production, proliferation and c-MYC mRNA expression in cancer cells. Next, we sought to evaluate the systemic impact of anti-insulin resistance treatments on our diabetic $HER2^{+}$ breast cancer mouse model. Since metformin is the first-line treatment for DM2, we expected metformin treatment to improve insulin resistance in MMTV-ErbB2/*Lepr*$^{db/db}$ mice (Figure 16). To further evaluate the systemic effect of anti-diabetic treatments *in vivo*, we performed a rat/mouse insulin ELISA assay. The level of insulin was 15-fold higher in the MMTV-ErbB2/*Lepr*$^{db/db}$ mice than in the MMTV-ErbB2/*Lepr*$^{+/+}$ mice ($P<0.001$), and dramatically decreasing in metformin and rosiglitazone treatment groups ($P<0.01$, Figure 17). This microenvironment change limited the insulin supply to the cancer cells and suppressed the mTOR/AKT signaling pathway in mouse tumors as shown by p-AKT-S473 and p-RPS6-S235/S236 (Figure 18).

DM2 is a severe metabolic disease and often comes with increased body weight and adipose tissue. Therefore, we sought to assess the adipokine profile changes in MMTV-ErbB2/*Lepr*$^{db/db}$ mice (Figure 19A), and more importantly, assess the profile upon anti-insulin resistance treatments (Figure 19B). Interestingly, we found that drug treatments reversed the impact of

DM2 on the expression level of Adiponectin, Fibroblast growth factor 1 (FGF1), Chemokine (C-C motif) ligand 2

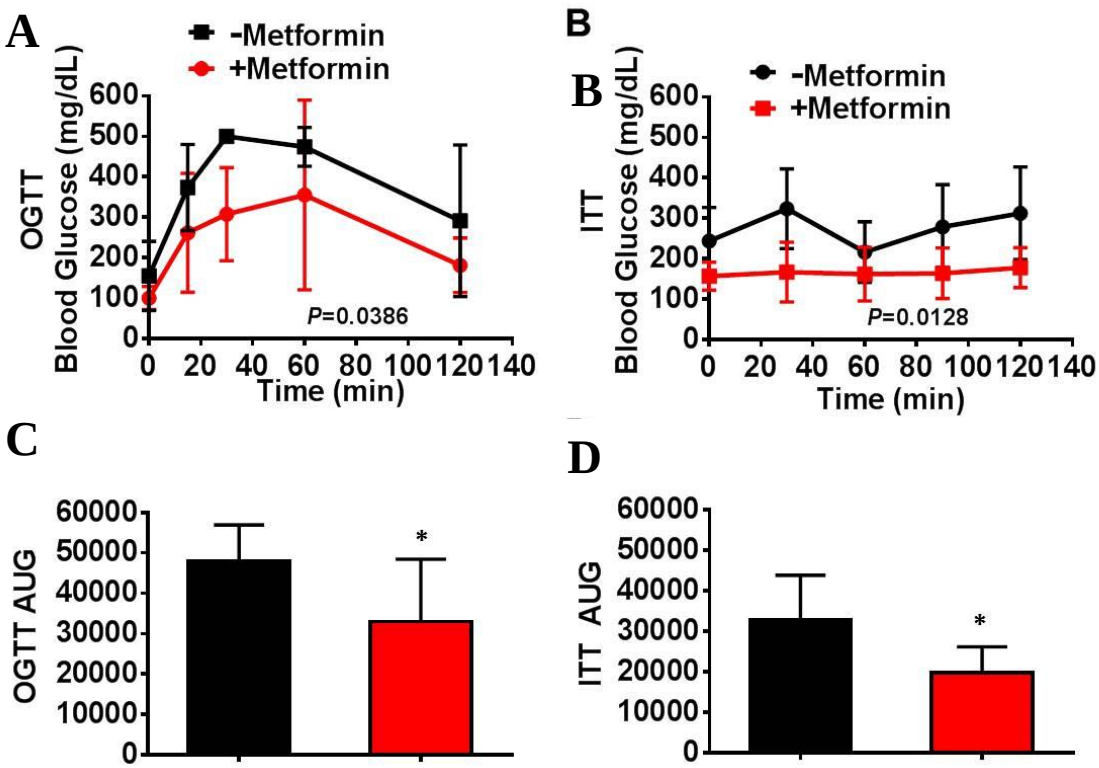

Figure 16. Metformin treatment improved type 2 diabetes in MMTV-ErbB2/*Lepr*$^{db/db}$ breast cancer mouse model

A) OGTT and B) ITT were performed on MMTV-ErbB2/*Lepr*$^{db/db}$ mice (n=4) before and after 2 weeks metformin treatment on the same mice. Area under the curve for C) OGTT and D) ITT was analyzed. Paired t-test was performed to show the significant difference. Values are means ± 95% CI.

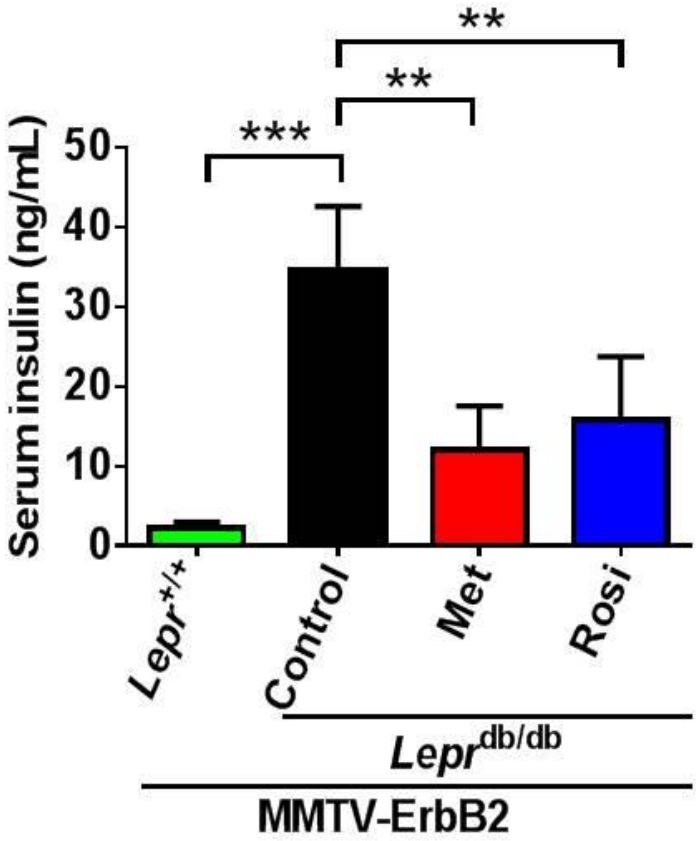

Figure 17. DM2 condition increases insulin levels and anti-insulin resistance treatments significantly reduce insulin levels in MMTV-ErbB2/*Lepr*$^{db/db}$ breast cancer mouse model

ELISA analysis for the serum insulin level was performed from different groups of mice. WT: MMTV-ErbB2/*Lepr*$^{+/+}$ mice=10; DB: MMTV-ErbB2/*Lepr*$^{db/db}$ mice/control=12; DB/Met: MMTV-ErbB2/*Lepr*$^{db/db}$ mice/metformin treatment=10; DB/Rosi: MMTV-ErbB2/*Lepr*$^{db/db}$ mice/rosiglitazone=16. Values are means ± 95% CI.

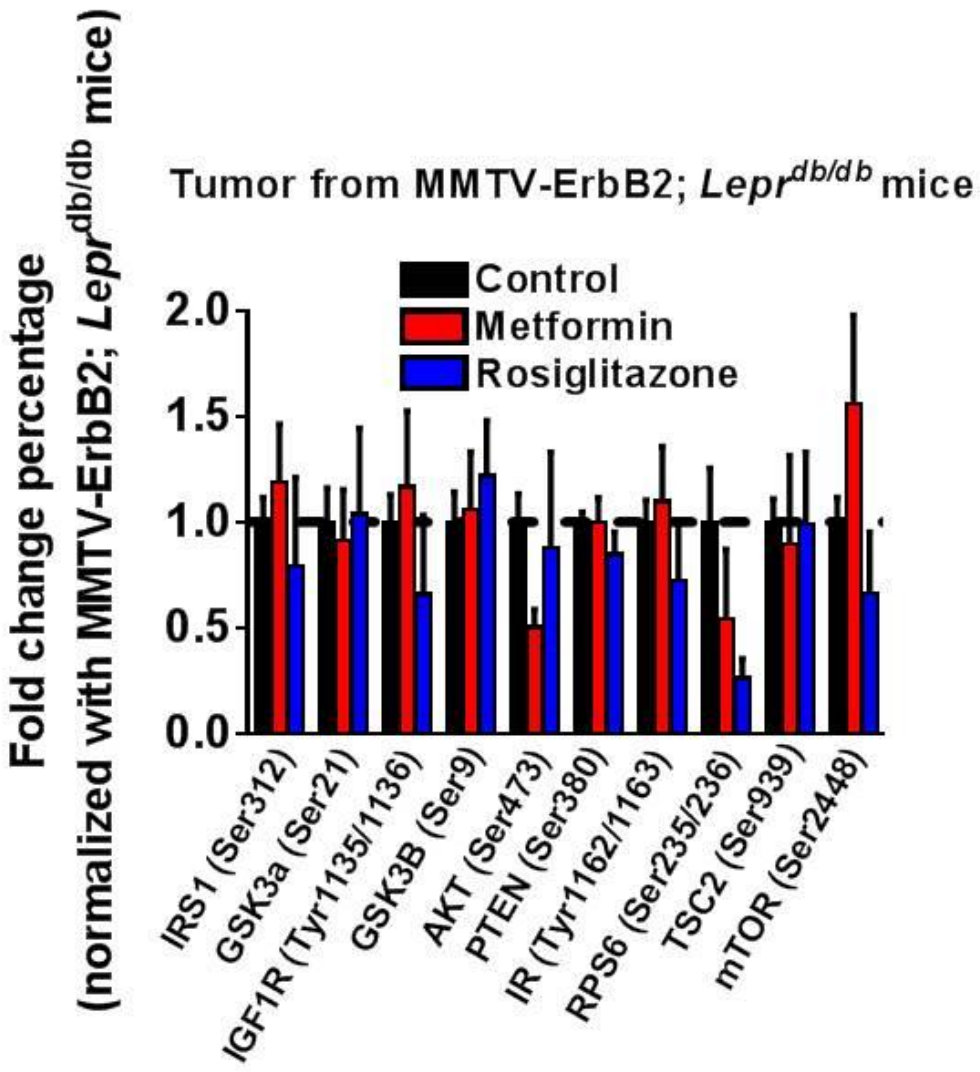

Figure 18. Multiplex analysis for mTOR/Akt signaling pathway

Tumors were harvested from MMTV-ErbB2/*Lepr*$^{db/db}$ mice treated with control (n=24), metformin (n=6), and rosiglitazone (n=6).

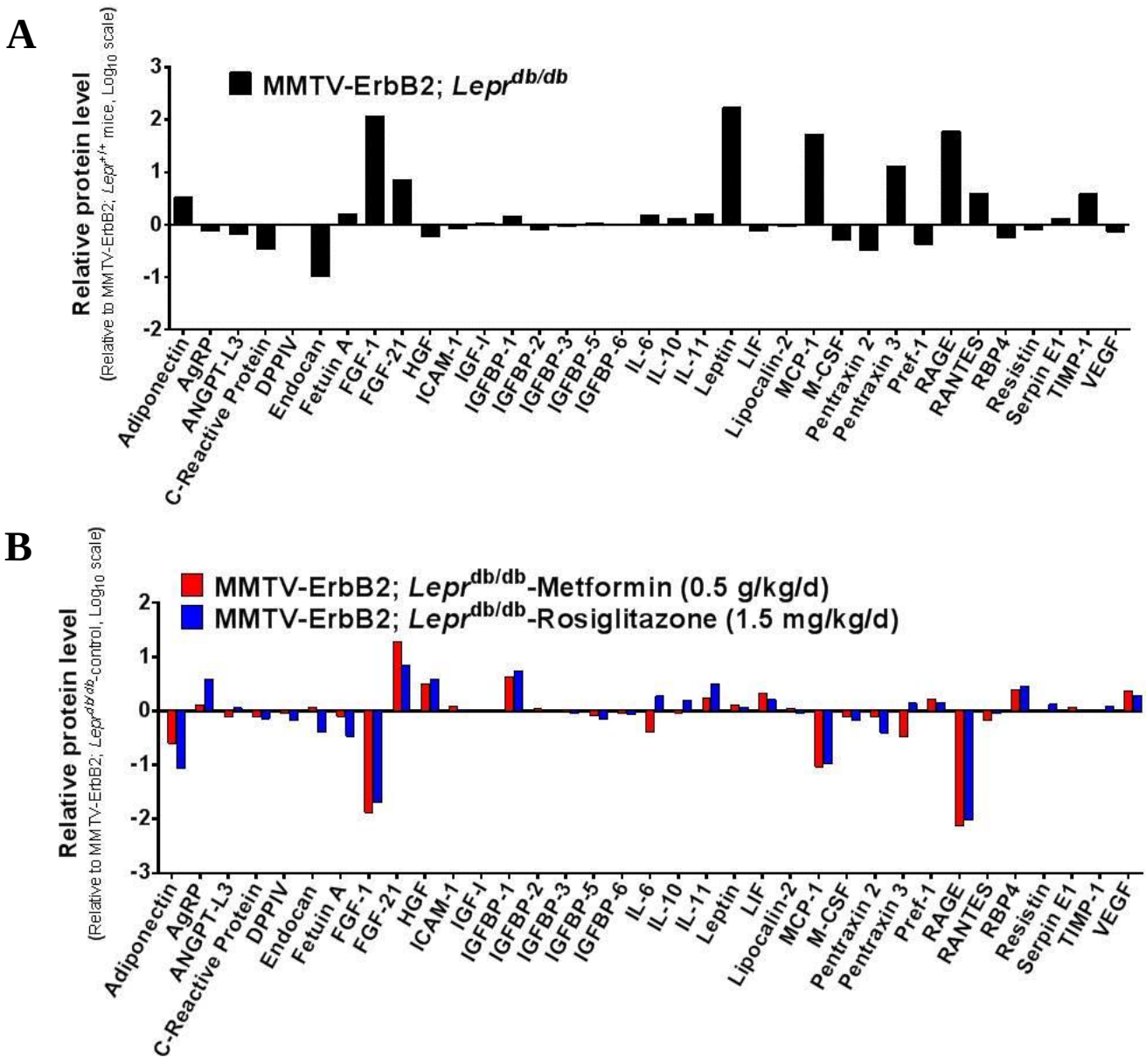

Figure 19. Adipokine expression profile in MMTV-ErbB2/*Lepr*$^{db/db}$ mice

A) Serum adipokine levels in MMTV-ErbB2/*Lepr*$^{db/db}$ mice comparing with MMTV-ErbB2/*Lepr*$^{+/+}$ mice. Serum samples from 3 mice of each group were mixed before incubating with adipokine array. **B)** Adipokine expression profile for MMTV-ErbB2/*Lepr*$^{db/db}$ mice treated with control, metformin, and rosiglitazone.

(MCP1) and receptor of advance glycosylation end products (RAGE). These adipokines may associate with anti-insulin resistance treatments and contribute to the beneficial impact on $HER2^+$ breast cancer progression.

CHAPTER 4. DISSCUSSION

Our findings suggest that DM2 promotes the progression of $HER2^+$ breast cancer, and this aggressiveness is attenuated by anti-insulin resistance treatments. We also successfully established a transgenic animal model and confirmed that the survival duration of mice with DM2 and $HER2^+$ breast cancer was shorter than that of control mice. Furthermore, by administrating anti-insulin resistance treatments to the diabetic $HER2^+$ breast cancer model, we demonstrated that metformin and rosiglitazone treatments significantly prolong overall survival and alter the metabolic status. All these results indicate the potential application of anti-insulin resistance treatments in $HER2^+$ breast cancer patients with DM2.

4.1 A successful DM2 $HER2^+$ breast cancer transgenic mouse model

Lepr$^{db/db}$ mice were discovered more than 40 years ago as an animal model in DM2 research (Belke and Severson, 2012; Hummel et al., 1966). Previous studies indicated that the *Lepr*$^{db/db}$ mouse model has deficient mammary gland development on a C57BL/6 genetic background. Cleary et al. (Cleary et al., 2004) and Zheng et al. (Zheng et al., 2011) also tried to cross MMTV-TGF-α mice or MMTV-Wnt-1 mice with *Lepr*$^{db/+}$ mice and maintain the mice on a C57BL/6 genetic background. They claimed that the leptin receptor deficiency suppressed the development of mammary tumors. However, the life expectancy of the MMTV-TGF-α mice or MMTV-Wnt-1 mice is longer than that of *Lepr*$^{db/db}$ mice, and the C57BL/6 genetic background is actually resistant to tumor progression in mouse models. In our study, we crossed our

transgenic mouse model in a tumor-prone FVB genetic background instead of a tumor-resistant C57BL/6 genetic background and found that DM2 promotes $HER2^{+}$ breast cancer progression. To our knowledge, we are the first group to successfully generate hyperinsulinemic, hyperglycemic, and obese MMTV-ErbB2/*Lepr*$^{db/db}$ mice. Therefore, we could use this animal model to assess the therapeutic effect of anti-insulin resistance agents.

4.2 Demonstrating the anti-cancer effect of anti-insulin resistance treatments by using clinical relevant concentration

Metformin is the most frequently prescribed anti-insulin resistance drug for DM2 patients, and many studies have shown that both metformin and rosiglitazone have anticancer activity. Studies showed that treatment with metformin and/or rosiglitazone inhibited cancer cell proliferation (Feng et al., 2011; Zhuang and Miskimins, 2008), induced cell apoptosis (Feng et al., 2011), selectively reduced cancer stem cell populations *in vitro (Hirsch et al., 2013; Hirsch et al., 2009)*, and attenuated cancer cell growth *in vivo (Anisimov et al., 2005a; Anisimov et al., 2005b; Fierz et al., 2013)*. However, none of these studies revealed alterations in breast cancer metabolism *in vivo*, and the majority studies of anti-insulin resistance treatments used either a high-fat diet or drugs to induce diabetes or the engraftment of tumor cells in the mice, which does not represent the true circumstances of cancer progression in the presence of DM2 in a transgenic setting. Moreover, the

majority of the studies were conducted by using metformin and/or rosiglitazone at concentrations that were not clinically relevant.

Other studies did not test these agents in an obese DM2 mouse model. Anisimov et al. showed the impact of metformin on tumor progression and survival in non-diabetic MMTV-ErbB2 mice (Anisimov et al., 2005a). Similarly, Fierz et al. established the effects of anti-diabetic drugs in a nonobese DM2 mouse model (Fierz et al., 2013). We sought to assess the effects of anti-insulin resistance treatments in the setting of $HER2^{+}$ breast cancer, DM2, and obesity. Therefore, we treated our MMTV-ErbB2/*Lepr*$^{db/db}$ mice with metformin or rosiglitazone at a clinical relevant concentration before palpable tumor formation and observed that tumor progression was significantly reduced and survival time was prolonged. In addition, the drugs did not inhibit tumor progression once the tumor had been established, indicating that the anti-diabetic drugs work better as cancer prevention agents (data not shown).

4.3 Real-time observation of anti-insulin resistance treatments alter breast cancer metabolism by directly inhibiting oxidative phosphorylation and glycolysis in vitro and in vivo

By assessing our MMTV-ErbB2/*Lepr*$^{db/db}$ mice with MRSI, we found that metformin or rosiglitazone treatments reduced cancer metabolism in the living mice. For this particular method, we monitored the glycolysis real-time *in vivo*. Interestingly, the rate at which ^{13}C-pyruvate was converted to ^{13}C-lactate was reduced significantly after 2 days of rosiglitazone treatment (Figure 12B), but not after 2 days

of metformin treatment (data not shown). The reduction in pyruvate/lactate conversion was found in the group treated with metformin for 2 weeks (Figure 12A), indicating that the physiologically relevant concentration of oral metformin may affect cancer metabolism only in a long-term treatment regimen. These results suggest that metformin and rosiglitazone regulate cancer metabolism via different mechanisms that need to be investigated.

Warburg effect is an important factor in cell metabolism (Vander Heiden et al., 2009; Warburg, 1956) and one of the hallmarks of cancer (Hanahan and Weinberg, 2011; Yeung et al., 2008). Regardless of whether oxygen is present, cancer cells tend to undergo aerobic glycolysis and convert most glucose to lactate instead of moving into TCA cycle. To confirm our observation *in vivo*, we isolated cancer cells from the primary tumor sites of MMTV-ErbB2/*Lepr*$^{db/db}$ mice and monitored the impact of metformin treatment directly on cancer cells. As a well-known mitochondrial complex I inhibitor (Owen et al., 2000), metformin at a clinically relevant concentration efficiently suppressed oxygen consumption, indicating that the mitochondrial respiratory chain reaction was repressed (Figure 13A). Although a previous study indicated that glycolysis increases when mitochondrial complex I is inhibited owing to the glycolysis flux (Brunmair et al., 2004), we observed that lactate production was decreased upon treatment with 300 μM metformin (Figure 13B), which is consistent with the MRSI finding. This result demonstrated that metformin may also affect multiple key components in the

glycolysis pathway, of which c-MYC is a primary regulator (Miller et al., 2012).

4.4 Metformin treatment inhibits c-MYC mRNA expression and induces c-MYC proteasome degradation

To expend our study closer to human, we selected two human $HER2^{+}$ breast cancer cell lines for our *in vitro* experiments. The proliferation of both BT-474 and MDA-MB-361 cells was inhibited at a clinically relevant concentration of metformin treatment (Figure 14A and 14B). However, metformin treatment induced apoptosis at a higher dose that was not a clinically relevant concentration (Figure 14C). c-MYC protein level was indeed decreasing upon metformin treatment. Additionally, the c-MYC downstream target PKM2, which is important for switching the metabolism to aerobic glycolysis (Christofk et al., 2008) was also repressed (Figure 14C and 15A). These findings may explain why there was no increase of lactate production when oxidative phosphorylation was inhibited. At the end, the glycolysis flux may have been blocked, and the metabolites may have been converted to phosphoenolpyruvate (PEP), 2-phosphoglycerate and 3-phosphoglycerate (2- and 3-PGA) as previous described (Owen et al., 2000). These intermediate metabolites are precursors for the pentose phosphate pathway (PPP) to synthesis nucleotides as building blocks for cancer cells. These accumulated intermediated metabolites also explain why metformin treatment can only postpone cancer progression but cannot eradicate it.

We next sought to determine the extent to which c-MYC is reduced at the transcriptional and/or post-translational level. Upon 500μM metformin treatment,

there was a significant difference at the c-MYC mRNA level (Figure 15A), suggesting that metformin may modulate c-MYC in a DICER-microRNA-33-c-MYC cascade according to previous findings (Blandino et al., 2012). In addition, c-MYC protein was restored to a comparable level in the presence of MG132, suggesting that metformin treatment was involved in c-MYC degradation (Figure 15B). For the ubiquitination assay, the endogenous c-MYC ubiquitination was first detected via immunoprecipitation with anti-ubiquitin antibody and then immunoblotted with anti-c-MYC antibody in BT-474 cells. The stacking gel was intentionally preserved, and Western blotting was performed for the whole gel. A highly ubiquitinated c-MYC was found in the stacking gel, and metformin treatment induced ubiquitination starting at 500 μM (Figure 15C). Although high concentrations of metformin treatment did not cause c-MYC ubiquitination in a dose-dependent manner in BT-474 cells, the clinically irrelevant concentrations may already disrupt and affect normal protein production in the cells. The c-MYC turnover rate was faster in the presence of 500 μM metformin (Figure 15D and E), supporting the notion that metformin treatment promotes c-MYC protein degradation.

4.5 Systematic effect of anti-insulin resistance treatments on breast cancer and microenvironment

Besides the impact of anti-insulin resistance treatments in cancer, we evaluated the systemic effects of the anti-insulin resistance treatments and the potential crosstalk between cancer cells and the microenvironment in our

diabetic HER2^{+} mouse model. The serum insulin level (Figure 17) was reduced, and insulin resistance was improved in MMTV-ErbB2/*Lepr*$^{db/db}$ mice (Figure S3) after anti-insulin resistance treatments. Although the downstream targets of insulin receptor signaling pathway and HER2 signaling pathway are overlap, anti-insulin resistance treatments prevented further stimulation from insulin and attenuated the mTOR/AKT signaling pathway (Figure 18), thereby gradually preventing cancer progression. In addition, by analyzing the adipokine profile, we identified the adipokines that were up-regulated under diabetic conditions (Figure 19A) and found adiponectin, FGF-1, MCP-1, and RAGE were significantly down-regulated by anti-insulin resistance treatments (Figure 19B). These four adipokines may serve as anti-cancer regulators in HER2^{+} breast cancer progression. This finding supports the idea that anti-insulin resistance treatments at clinically relevant concentration not only altered cancer cell metabolism but also rendered the microenvironment unfavorable to tumor progression in our diabetic HER2^{+} breast cancer mouse model.

In conclusion, we established a new animal model to assess the impact of DM2 on breast cancer progression and showed that anti-insulin resistance treatments may delay tumor onset and retard cancer progression in MMTV-ErbB2/*Lepr*$^{db/db}$ mice. The treatments not only stopped proliferation and altered metabolism in cancer cells but also changed the microenvironment through systemic regulation of insulin levels and adipokine expression. To take bench research to the bedside, these results suggest that anti-diabetic drugs may be used as cancer prevention agents for diabetic patients who have increased risk of HER2^{+} breast cancer.

4.6 Future direction

It had been shown that metformin and rosiglitazone react through distinct pathway (Fryer et al., 2002). Our data ^{13}C-pyruvate data showed that metformin required longer treatment (2 weeks) to be able to reduced lactate/pyruvate conversion, while rosiglitazone only needed 2 days to achieve the inhibition. In addition, metformin treatment also inhibited alanine to pyruvate conversion (5.99%) while rosiglitazone actually increased it (175.68%) (data not shown). These data suggest that metformin not only inhibits glycolysis, it may also inhibit amino acids synthesis as building blocks for cancer cells. If metformin treatment is able to inhibit oxidative phosphorylation, aerobic glycolysis, and amino acid synthesis at the same time, where the glucose metabolites go? Previous study showed that an intermediate of the de novo purine nucleotide synthesis pathway, SAICAR (succinylaminoimidazolecarboxamide ribose-5'-phosphate), was involved in regulating PKM2 and was able to promote cancer cell survival (Keller et al., 2012). To find the metabolites that potentially keep cancer cell survive may be the key to cure breast cancer.

In our study, we found that metformin treatment induces c-MYC proteasome degradation. However, what mechanism and which E3 ligase is involved needs to be clarified. I previously identified that Pin1 phosphorylation at serine 71 is necessary to form the 14-3-3σ-pin1-MYC complex and mediated c-MYC degradation. It will be interesting to see

whether metformin treatment increases Pin1 or 14-3-3σ protein levels or stimulates PIN1 S71 phosphorylation.

We identified FGF1, MCP1 and RAGE could be the potential anti-cancer adipokines as therapeutic options for drug development. For example, MCP1 is a monocyte chemoattractant protein which may involve in the monocyte infiltration as cancer progress. Since metformin and rosiglitazone can inhibit the inflammatory response (Hirsch et al., 2013; Yki-Jarvinen, 2004), it is very interesting to know how anti-insulin resistance treatments can inhibit MCP1 secretion. I previously tried to link the reduction of MCP1 by using cancer cells as the model but failed. However, the MCP1 reduction could be the effect of drug treatments on microenvironment. Therefore, the direction should focus on adipocytes or stromal cells instead of cancer cells. In conclusion, solving these underlying questions may lead us to find new therapeutic targets for breast cancer.

CHAPTER 5. BIBLIOGRAPHY

American Cancer Society, I. (2014). Cancer Facts & Figures.

American Diabetes Association, I. (2011). Diagnosis and classification of diabetes mellitus. Diabetes Care *34 Suppl 1*, S62-69.

Anisimov, V.N., Berstein, L.M., Egormin, P.A., Piskunova, T.S., Popovich, I.G., Zabezhinski, M.A., Kovalenko, I.G., Poroshina, T.E., Semenchenko, A.V., Provinciali, M., *et al.* (2005a). Effect of metformin on life span and on the development of spontaneous mammary tumors in HER-2/neu transgenic mice. Exp Gerontol *40*, 685-693.

Anisimov, V.N., Egormin, P.A., Bershtein, L.M., Zabezhinskii, M.A., Piskunova, T.S., Popovich, I.G., and Semenchenko, A.V. (2005b). Metformin decelerates aging and development of mammary tumors in HER-2/neu transgenic mice. Bull Exp Biol Med *139*, 721-723.

Belke, D.D., and Severson, D.L. (2012). Diabetes in mice with monogenic obesity: the db/db mouse and its use in the study of cardiac consequences. Methods Mol Biol *933*, 47-57.

Ben Sahra, I., Laurent, K., Loubat, A., Giorgetti-Peraldi, S., Colosetti, P., Auberger, P., Tanti, J.F., Le Marchand-Brustel, Y., and Bost, F. (2008). The antidiabetic drug

metformin exerts an antitumoral effect in vitro and in vivo through a decrease of cyclin D1 level. Oncogene *27*, 3576-3586.

Blandino, G., Valerio, M., Cioce, M., Mori, F., Casadei, L., Pulito, C., Sacconi, A., Biagioni, F., Cortese, G., Galanti, S., *et al.* (2012). Metformin elicits anticancer effects through the sequential modulation of DICER and c-MYC. Nat Commun *3*, 865.

Bowker, S.L., Majumdar, S.R., Veugelers, P., and Johnson, J.A. (2006). Increased cancer-related mortality for patients with type 2 diabetes who use sulfonylureas or insulin: Response to Farooki and Schneider. Diabetes Care *29*, 1990-1991.

Bren-Mattison, Y., Meyer, A.M., Van Putten, V., Li, H., Kuhn, K., Stearman, R., Weiser-Evans, M., Winn, R.A., Heasley, L.E., and Nemenoff, R.A. (2008). Antitumorigenic effects of peroxisome proliferator-activated receptor-gamma in non-small-cell lung cancer cells are mediated by suppression of cyclooxygenase-2 via inhibition of nuclear factor-kappaB. Mol Pharmacol *73*, 709-717.

Bren-Mattison, Y., Van Putten, V., Chan, D., Winn, R., Geraci, M.W., and Nemenoff, R.A. (2005). Peroxisome proliferator-activated receptor-gamma (PPAR(gamma)) inhibits tumorigenesis by reversing the undifferentiated phenotype of metastatic non-small-cell lung cancer cells (NSCLC). Oncogene *24*, 1412-1422.

Brunmair, B., Gras, F., Neschen, S., Roden, M., Wagner, L., Waldhausl, W., and Furnsinn, C. (2001). Direct thiazolidinedione action on isolated rat skeletal muscle fuel handling is independent of peroxisome proliferator-activated receptor-gamma-mediated changes in gene expression. Diabetes *50*, 2309-2315.

Brunmair, B., Staniek, K., Gras, F., Scharf, N., Althaym, A., Clara, R., Roden, M., Gnaiger, E., Nohl, H., Waldhausl, W., *et al.* (2004). Thiazolidinediones, like metformin, inhibit respiratory complex I: a common mechanism contributing to their antidiabetic actions? Diabetes *53*, 1052-1059.

Butler, P.C. (2009). Insulin glargine controversy: a tribute to the editorial team at Diabetologia. Diabetes *58*, 2427-2428.

Buzzai, M., Jones, R.G., Amaravadi, R.K., Lum, J.J., DeBerardinis, R.J., Zhao, F., Viollet, B., and Thompson, C.B. (2007). Systemic treatment with the antidiabetic drug metformin selectively impairs p53-deficient tumor cell growth. Cancer Res *67*, 6745-6752.

Cao, L.Q., Chen, X.L., Wang, Q., Huang, X.H., Zhen, M.C., Zhang, L.J., Li, W., and Bi, J. (2007). Upregulation of PTEN involved in rosiglitazone-induced apoptosis in human hepatocellular carcinoma cells. Acta Pharmacol Sin *28*, 879-887.

Carey, L.A., Perou, C.M., Livasy, C.A., Dressler, L.G., Cowan, D., Conway, K., Karaca, G., Troester, M.A., Tse, C.K., Edmiston, S., *et al.* (2006). Race, breast cancer subtypes, and survival in the Carolina Breast Cancer Study. JAMA *295*, 2492-2502.

Centers for Disease Control and Prevention. National Center for Chronic Disease Prevention and Health Promotion. Diabetes at A Glance. Atlanta (2011). GA: U.S. Department of Health and Human Services, Centers for Disease Control and Prevention.

Chang, C.H., Lin, J.W., Wu, L.C., Lai, M.S., Chuang, L.M., and Chan, K.A. (2012). Association of thiazolidinediones with liver cancer and colorectal cancer in type 2 diabetes mellitus. Hepatology *55*, 1462-1472.

Christofk, H.R., Vander Heiden, M.G., Harris, M.H., Ramanathan, A., Gerszten, R.E., Wei, R., Fleming, M.D., Schreiber, S.L., and Cantley, L.C. (2008). The M2 splice isoform of pyruvate kinase is important for cancer metabolism and tumour growth. Nature *452*, 230-233.

Cleary, M.P., Juneja, S.C., Phillips, F.C., Hu, X., Grande, J.P., and Maihle, N.J. (2004). Leptin receptor-deficient MMTV-TGF-alpha/Lepr(db)Lepr(db) female mice do not develop oncogene-induced mammary tumors. Exp Biol Med (Maywood) *229*, 182-193.

Colhoun, H.M. (2009). Use of insulin glargine and cancer incidence in Scotland: a study from the Scottish Diabetes Research Network Epidemiology Group. Diabetologia *52*, 1755-1765.

Creighton, C.J., Li, X., Landis, M., Dixon, J.M., Neumeister, V.M., Sjolund, A., Rimm, D.L., Wong, H., Rodriguez, A., Herschkowitz, J.I., *et al.* (2009). Residual breast cancers after conventional therapy display mesenchymal as well as tumor-initiating features. Proc Natl Acad Sci U S A *106*, 13820-13825.

Cryer, D.R., Nicholas, S.P., Henry, D.H., Mills, D.J., and Stadel, B.V. (2005). Comparative outcomes study of metformin intervention versus conventional approach the COSMIC Approach Study. Diabetes Care *28*, 539-543.

Day, S.E., Kettunen, M.I., Gallagher, F.A., Hu, D.E., Lerche, M., Wolber, J., Golman, K., Ardenkjaer-Larsen, J.H., and Brindle, K.M. (2007). Detecting tumor response to treatment using hyperpolarized 13C magnetic resonance imaging and spectroscopy. Nat Med *13*, 1382-1387.

Dezaki, K., Hosoda, H., Kakei, M., Hashiguchi, S., Watanabe, M., Kangawa, K., and Yada, T. (2004). Endogenous ghrelin in pancreatic islets restricts insulin release by attenuating Ca2+ signaling in beta-cells: implication in the glycemic control in rodents. Diabetes *53*, 3142-3151.

DiGiovanni, J., Bhatt, T.S., and Walker, S.E. (1993). C57BL/6 mice are resistant to tumor promotion by full thickness skin wounding. Carcinogenesis *14*, 319-321.

Drinkwater, N.R., and Ginsler, J.J. (1986). Genetic control of hepatocarcinogenesis in C57BL/6J and C3H/HeJ inbred mice. Carcinogenesis *7*, 1701-1707.

Fan, C., Oh, D.S., Wessels, L., Weigelt, B., Nuyten, D.S., Nobel, A.B., van't Veer, L.J., and Perou, C.M. (2006). Concordance among gene-expression-based predictors for breast cancer. N Engl J Med *355*, 560-569.

Feng, Y.H., Velazquez-Torres, G., Gully, C., Chen, J., Lee, M.H., and Yeung, S.C. (2011). The impact of type 2 diabetes and antidiabetic drugs on cancer cell growth. J Cell Mol Med *15*, 825-836.

Fierz, Y., Novosyadlyy, R., Vijayakumar, A., Yakar, S., and LeRoith, D. (2013). Insulin-sensitizing therapy attenuates type 2 diabetes-mediated mammary tumor progression. Diabetes *59*, 686-693.

Fischer, S.M., Jasheway, D.W., Klann, R.C., Butler, A.P., Patrick, K.E., Baldwin, J.K., and Cameron, G.S. (1989). Correlation of phorbol ester promotion in the resistant C57BL/6J mouse with sustained hyperplasia but not ornithine decarboxylase or protein kinase C. Cancer Res *49*, 6693-6699.

Foretz, M., Hebrard, S., Leclerc, J., Zarrinpashneh, E., Soty, M., Mithieux, G., Sakamoto, K., Andreelli, F., and Viollet, B. (2010). Metformin inhibits hepatic gluconeogenesis in mice independently of the LKB1/AMPK pathway via a decrease in hepatic energy state. J Clin Invest *120*, 2355-2369.

Fryer, L.G., Parbu-Patel, A., and Carling, D. (2002). The Anti-diabetic drugs rosiglitazone and metformin stimulate AMP-activated protein kinase through distinct signaling pathways. J Biol Chem *277*, 25226-25232.

Giovannucci, E., Harlan, D.M., Archer, M.C., Bergenstal, R.M., Gapstur, S.M., Habel, L.A., Pollak, M., Regensteiner, J.G., and Yee, D. (2010). Diabetes and cancer: a consensus report. Diabetes Care *33*, 1674-1685.

Girnun, G.D., Naseri, E., Vafai, S.B., Qu, L., Szwaya, J.D., Bronson, R., Alberta, J.A., and Spiegelman, B.M. (2007). Synergy between PPARgamma ligands and platinum-based drugs in cancer. Cancer Cell *11*, 395-406.

Goldhirsch, A., Wood, W.C., Coates, A.S., Gelber, R.D., Thurlimann, B., and Senn, H.J. (2011). Strategies for subtypes--dealing with the diversity of breast cancer: highlights of the St. Gallen International Expert Consensus on the Primary Therapy of Early Breast Cancer 2011. Ann Oncol *22*, 1736-1747.

Golman, K., Zandt, R.I., Lerche, M., Pehrson, R., and Ardenkjaer-Larsen, J.H. (2006). Metabolic imaging by hyperpolarized 13C magnetic resonance imaging for in vivo tumor diagnosis. Cancer Res *66*, 10855-10860.

Graham, D.J., and Gelperin, K. (2010). FDA on rosiglitazone. More on advisory committee decision. BMJ *341*, c4868.

Graham, D.J., Ouellet-Hellstrom, R., MaCurdy, T.E., Ali, F., Sholley, C., Worrall, C., and Kelman, J.A. (2010). Risk of acute myocardial infarction, stroke, heart failure, and death in elderly Medicare patients treated with rosiglitazone or pioglitazone. JAMA *304*, 411-418.

Gunton, J.E., Delhanty, P.J., Takahashi, S., and Baxter, R.C. (2003). Metformin rapidly increases insulin receptor activation in human liver and signals preferentially through insulin-receptor substrate-2. J Clin Endocrinol Metab *88*, 1323-1332.

Han, S., and Roman, J. (2006). Rosiglitazone suppresses human lung carcinoma cell growth through PPARgamma-dependent and PPARgamma-independent signal pathways. Mol Cancer Ther *5*, 430-437.

Han, S., Sidell, N., Fisher, P.B., and Roman, J. (2004). Up-regulation of p21 gene expression by peroxisome proliferator-activated receptor gamma in human lung carcinoma cells. Clin Cancer Res *10*, 1911-1919.

Hanahan, D., and Weinberg, R.A. (2011). Hallmarks of cancer: the next generation. Cell *144*, 646-674.

He, X., Esteva, F.J., Ensor, J., Hortobagyi, G.N., Lee, M.H., and Yeung, S.C. (2012). Metformin and thiazolidinediones are associated with improved breast cancer-specific survival of diabetic women with HER2+ breast cancer. Ann Oncol *23*, 1771-1780.

Hemkens, L.G., Grouven, U., Bender, R., Gunster, C., Gutschmidt, S., Selke, G.W., and Sawicki, P.T. (2009). Risk of malignancies in patients with diabetes treated with human insulin or insulin analogues: a cohort study. Diabetologia *52*, 1732-1744.

Herschkowitz, J.I., Simin, K., Weigman, V.J., Mikaelian, I., Usary, J., Hu, Z., Rasmussen, K.E., Jones, L.P., Assefnia, S., Chandrasekharan, S., *et al.* (2007). Identification of conserved gene expression features between murine mammary carcinoma models and human breast tumors. Genome Biol *8*, R76.

Hirsch, H.A., Iliopoulos, D., and Struhl, K. (2013). Metformin inhibits the inflammatory response associated with cellular transformation and cancer stem cell growth. Proc Natl Acad Sci U S A *110*, 972-977.

Hirsch, H.A., Iliopoulos, D., Tsichlis, P.N., and Struhl, K. (2009). Metformin selectively targets cancer stem cells, and acts together with chemotherapy to block tumor growth and prolong remission. Cancer Res *69*, 7507-7511.

Home, P.D., Pocock, S.J., Beck-Nielsen, H., Gomis, R., Hanefeld, M., Jones, N.P., Komajda, M., and McMurray, J.J. (2007). Rosiglitazone evaluated for cardiovascular outcomes--an interim analysis. N Engl J Med *357*, 28-38.

Hummel, K.P., Dickie, M.M., and Coleman, D.L. (1966). Diabetes, a new mutation in the mouse. Science *153*, 1127-1128.

Keller, K.E., Tan, I.S., and Lee, Y.S. (2012). SAICAR stimulates pyruvate kinase isoform M2 and promotes cancer cell survival in glucose-limited conditions. Science *338*, 1069-1072.

Keshamouni, V.G., Arenberg, D.A., Reddy, R.C., Newstead, M.J., Anthwal, S., and Standiford, T.J. (2005). PPAR-gamma activation inhibits angiogenesis by blocking ELR+CXC chemokine production in non-small cell lung cancer. Neoplasia *7*, 294-301.

Lee, S.Y., Hur, G.Y., Jung, K.H., Jung, H.C., Kim, J.H., Shin, C., Shim, J.J., In, K.H., Kang, K.H., and Yoo, S.H. (2006). PPAR-gamma agonist increase gefitinib's antitumor activity through PTEN expression. Lung Cancer *51*, 297-301.

Lehmann, J.M., Moore, L.B., Smith-Oliver, T.A., Wilkison, W.O., Willson, T.M., and Kliewer, S.A. (1995). An antidiabetic thiazolidinedione is a high affinity ligand for peroxisome proliferator-activated receptor gamma (PPAR gamma). J Biol Chem *270*, 12953-12956.

Maehama, T., and Dixon, J.E. (1998). The tumor suppressor, PTEN/MMAC1, dephosphorylates the lipid second messenger, phosphatidylinositol 3,4,5-trisphosphate. J Biol Chem *273*, 13375-13378.

McIntyre, H.D., Ma, A., Bird, D.M., Paterson, C.A., Ravenscroft, P.J., and Cameron, D.P. (1991). Metformin increases insulin sensitivity and basal glucose clearance in type 2 (non-insulin dependent) diabetes mellitus. Aust N Z J Med *21*, 714-719.

Miller, D.M., Thomas, S.D., Islam, A., Muench, D., and Sedoris, K. (2012). c-Myc and cancer metabolism. Clin Cancer Res *18*, 5546-5553.

Miller, R.A., Chu, Q., Xie, J., Foretz, M., Viollet, B., and Birnbaum, M.J. (2013). Biguanides suppress hepatic glucagon signalling by decreasing production of cyclic AMP. Nature *494*, 256-260.

Mitka, M. (2013). Panel recommends easing restrictions on rosiglitazone despite concerns about cardiovascular safety. JAMA *310*, 246-247.

Monami, M., Dicembrini, I., and Mannucci, E. (2014). Thiazolidinediones and cancer: results of a meta-analysis of randomized clinical trials. Acta Diabetol *51*, 91-101.

Monami, M., Lamanna, C., Balzi, D., Marchionni, N., and Mannucci, E. (2009). Sulphonylureas and cancer: a case-control study. Acta Diabetol *46*, 279-284.

Monami, M., Lamanna, C., Marchionni, N., and Mannucci, E. (2008). Rosiglitazone and risk of cancer: a meta-analysis of randomized clinical trials. Diabetes Care *31*, 1455-1460.

Narayan, K.M., Boyle, J.P., Thompson, T.J., Sorensen, S.W., and Williamson, D.F. (2003). Lifetime risk for diabetes mellitus in the United States. JAMA *290*, 1884-1890.

Nissen, S.E., and Wolski, K. (2007). Effect of rosiglitazone on the risk of myocardial infarction and death from cardiovascular causes. N Engl J Med *356*, 2457-2471.

Ohta, K., Endo, T., Haraguchi, K., Hershman, J.M., and Onaya, T. (2001). Ligands for peroxisome proliferator-activated receptor gamma inhibit growth and induce apoptosis of human papillary thyroid carcinoma cells. J Clin Endocrinol Metab *86*, 2170-2177.

Owen, M.R., Doran, E., and Halestrap, A.P. (2000). Evidence that metformin exerts its anti-diabetic effects through inhibition of complex 1 of the mitochondrial respiratory chain. Biochem J *348 Pt 3*, 607-614.

Patel, L., Pass, I., Coxon, P., Downes, C.P., Smith, S.A., and Macphee, C.H. (2001). Tumor suppressor and anti-inflammatory actions of PPARgamma agonists are mediated via upregulation of PTEN. Curr Biol *11*, 764-768.

Perou, C.M., and Borresen-Dale, A.L. (2011). Systems biology and genomics of breast cancer. Cold Spring Harb Perspect Biol *3*.

Perou, C.M., Sorlie, T., Eisen, M.B., van de Rijn, M., Jeffrey, S.S., Rees, C.A., Pollack, J.R., Ross, D.T., Johnsen, H., Akslen, L.A., *et al.* (2000). Molecular portraits of human breast tumours. Nature *406*, 747-752.

Piccart-Gebhart, M.J., Procter, M., Leyland-Jones, B., Goldhirsch, A., Untch, M., Smith, I., Gianni, L., Baselga, J., Bell, R., Jackisch, C., *et al.* (2005). Trastuzumab after adjuvant chemotherapy in HER2-positive breast cancer. N Engl J Med *353*, 1659-1672.

Prat, A., Parker, J.S., Karginova, O., Fan, C., Livasy, C., Herschkowitz, J.I., He, X., and Perou, C.M. (2010). Phenotypic and molecular characterization of the claudin-low intrinsic subtype of breast cancer. Breast Cancer Res *12*, R68.

Prat, A., and Perou, C.M. (2009). Mammary development meets cancer genomics. Nat Med *15*, 842-844.

Prat, A., and Perou, C.M. (2011). Deconstructing the molecular portraits of breast cancer. Mol Oncol *5*, 5-23.

Reis-Filho, J.S., and Pusztai, L. (2011). Gene expression profiling in breast cancer: classification, prognostication, and prediction. Lancet *378*, 1812-1823.

Ross, J.S., Fletcher, J.A., Linette, G.P., Stec, J., Clark, E., Ayers, M., Symmans, W.F., Pusztai, L., and Bloom, K.J. (2003). The Her-2/neu gene and protein in breast cancer 2003: biomarker and target of therapy. Oncologist *8*, 307-325.

Rowse, G.J., Ritland, S.R., and Gendler, S.J. (1998). Genetic modulation of neu proto-oncogene-induced mammary tumorigenesis. Cancer Res *58*, 2675-2679.

Salpeter, S.R., Greyber, E., Pasternak, G.A., and Salpeter, E.E. (2003). Risk of fatal and nonfatal lactic acidosis with metformin use in type 2 diabetes mellitus: systematic review and meta-analysis. Arch Intern Med *163*, 2594-2602.

Shaw, R.J., Lamia, K.A., Vasquez, D., Koo, S.H., Bardeesy, N., Depinho, R.A., Montminy, M., and Cantley, L.C. (2005). The kinase LKB1 mediates glucose homeostasis in liver and therapeutic effects of metformin. Science *310*, 1642-1646.

Shu, Y., Sheardown, S.A., Brown, C., Owen, R.P., Zhang, S., Castro, R.A., Ianculescu, A.G., Yue, L., Lo, J.C., Burchard, E.G., *et al.* (2007). Effect of genetic variation in the organic cation transporter 1 (OCT1) on metformin action. J Clin Invest *117*, 1422-1431.

Sorlie, T., Tibshirani, R., Parker, J., Hastie, T., Marron, J.S., Nobel, A., Deng, S., Johnsen, H., Pesich, R., Geisler, S., *et al.* (2003). Repeated observation of breast tumor subtypes in independent gene expression data sets. Proc Natl Acad Sci U S A *100*, 8418-8423.

Sotiriou, C., Neo, S.Y., McShane, L.M., Korn, E.L., Long, P.M., Jazaeri, A., Martiat, P., Fox, S.B., Harris, A.L., and Liu, E.T. (2003). Breast cancer classification and prognosis based on gene expression profiles from a population-based study. Proc Natl Acad Sci U S A *100*, 10393-10398.

Vander Heiden, M.G., Cantley, L.C., and Thompson, C.B. (2009). Understanding the Warburg effect: the metabolic requirements of cell proliferation. Science *324*, 1029-1033.

Vargo-Gogola, T., and Rosen, J.M. (2007). Modelling breast cancer: one size does not fit all. Nat Rev Cancer *7*, 659-672.

Voduc, K.D., Cheang, M.C., Tyldesley, S., Gelmon, K., Nielsen, T.O., and Kennecke, H. (2010). Breast cancer subtypes and the risk of local and regional relapse. J Clin Oncol *28*, 1684-1691.

Warburg, O. (1956). On the origin of cancer cells. Science *123*, 309-314.

Wiholm, B.E., and Myrhed, M. (1993). Metformin-associated lactic acidosis in Sweden 1977-1991. Eur J Clin Pharmacol *44*, 589-591.

Yeung, S.J., Pan, J., and Lee, M.H. (2008). Roles of p53, MYC and HIF-1 in regulating glycolysis - the seventh hallmark of cancer. Cell Mol Life Sci *65*, 3981-3999.

Yki-Jarvinen, H. (2004). Thiazolidinediones. N Engl J Med *351*, 1106-1118.

Zheng, Q., Dunlap, S.M., Zhu, J., Downs-Kelly, E., Rich, J., Hursting, S.D., Berger, N.A., and Reizes, O. (2011). Leptin deficiency suppresses MMTV-Wnt-1 mammary tumor growth in obese mice and abrogates tumor initiating cell survival. Endocr Relat Cancer *18*, 491-503.

Zhou, G., Myers, R., Li, Y., Chen, Y., Shen, X., Fenyk-Melody, J., Wu, M., Ventre, J., Doebber, T., Fujii, N., *et al.* (2001). Role of AMP-activated protein kinase in mechanism of metformin action. J Clin Invest *108*, 1167-1174.

Zhu, Z., Jiang, W., Thompson, M.D., McGinley, J.N., and Thompson, H.J. (2011). Metformin as an energy restriction mimetic agent for breast cancer prevention. J Carcinog *10*, 17.

Zhuang, Y., and Miskimins, W.K. (2008). Cell cycle arrest in Metformin treated breast cancer cells involves activation of AMPK, downregulation of cyclin D1, and requires p27Kip1 or p21Cip1. J Mol Signal *3*, 18.

Zou, W., Liu, X., Yue, P., Khuri, F.R., and Sun, S.Y. (2007). PPARgamma ligands enhance TRAIL-induced apoptosis through DR5 upregulation and c-FLIP downregulation in human lung cancer cells. Cancer Biol Ther *6*, 99-106.

Vita

Ping-Chieh Benjamin Chou was born in Kaohsiung, Taiwan on January 10, 1977, the son of Tzu-Ling Chu and Kao-Chung Chou. After he received the degree of Bachelor of Science with a major in Animal Science from Tunghai University in May, 2000, he took his next step into Molecular Biology and received a Master degree in May, 2002. Houston, Texas. After he served in the army for 2 years, he came to the United States as a research assistant in the Department of Human Genetics at Baylor College of Medicine. In May of 2007 he entered The University of Texas Graduate School of Biomedical Sciences at Houston pursuing his doctor of philosophy degree in cancer biology.

Permanent address:

2F, No.9, Alley 29, Lane 120,

Nanking E. Rd. Sec 4, Taipei, Taiwan, R.O.C.